

NAVAL POSTGRADUATE SCHOOL

Monterey, California



19980505 066

THESIS

DTIC QUALITY INSPECTED 4

DEVELOPMENT AND CALIBRATION OF A TORSIONAL ENGINE MODEL FOR A THREE- CYLINDER, TWO-STROKE DIESEL ENGINE

by

James W. Hudson

December, 1997

Thesis Advisor:

Knox T. Millsaps, Jr.

Approved for public release; distribution is unlimited.

REPORT DOCUMENTATION PAGE

Form Approved OMB No. 0704-0188

Public reporting burden for this collection of information is estimated to average 1 hour per response, including the time for reviewing instruction, searching existing data sources, gathering and maintaining the data needed, and completing and reviewing the collection of information. Send comments regarding this burden estimate or any other aspect of this collection of information, including suggestions for reducing this burden, to Washington Headquarters Services, Directorate for Information Operations and Reports, 1215 Jefferson Davis Highway, Suite 1204, Arlington, VA 22202-4302, and to the Office of Management and Budget, Paperwork Reduction Project (0704-0188) Washington DC 20503.

1. AGENCY USE ONLY <i>(Leave blank)</i>	2. REPORT DATE December 1997	3. REPORT TYPE AND DATES COVERED Master's Thesis	
4. DEVELOPMENT AND CALIBRATION OF A TORSIONAL ENGINE MODEL FOR A THREE-CYLINDER, TWO-STROKE DIESEL ENGINE		5. FUNDING NUMBERS	
6. AUTHOR(S) James W. Hudson			
7. PERFORMING ORGANIZATION NAME(S) AND ADDRESS(ES) Naval Postgraduate School Monterey CA 93943-5000		8. PERFORMING ORGANIZATION REPORT NUMBER	
9. SPONSORING/MONITORING AGENCY NAME(S) AND ADDRESS(ES)		10. SPONSORING/MONITORING AGENCY REPORT NUMBER	
11. SUPPLEMENTARY NOTES The views expressed in this thesis are those of the author and do not reflect the official policy or position of the Department of Defense or the U.S. Government.			
12a. DISTRIBUTION/AVAILABILITY STATEMENT Approved for public release; distribution is unlimited.		12b. DISTRIBUTION CODE	
13. ABSTRACT <i>(maximum 200 words)</i> An experimental and analytical investigation was conducted to develop a calibrated torsional model of a three-cylinder, two-stroke diesel engine. A Detroit Diesel 3-53 engine was instrumented for time resolved measurement of cylinder firing pressures and high resolution near instantaneous shaft speed using a 720 and a 3,600 count per revolution optical encoder. Data were taken for three speeds and three torques for a total of nine conditions. A six degree-of-freedom torsional vibration model of the crankshaft, connecting rods, and pistons was developed. The nonlinear inertias, due to the reciprocating pistons, were included along with linear stiffness and damping. The equations of motion were numerically integrated over a cycle to obtain predicted response. The predicted response was compared to the measured response at the free end of the crankshaft.			
14. SUBJECT TERMS: diesel, torsional vibration model, cylinder pressure prediction		15. NUMBER OF PAGES: 74	
		16. PRICE CODE	
17. SECURITY CLASSIFICATION OF REPORT Unclassified	18. SECURITY CLASSIFICATION OF THIS PAGE Unclassified	19. SECURITY CLASSIFICATION OF ABSTRACT Unclassified	20. LIMITATION OF ABSTRACT UL

Approved for public release; distribution is unlimited

**DEVELOPMENT AND CALIBRATION OF A TORSIONAL ENGINE
MODEL FOR A THREE-CYLINDER, TWO-STROKE DIESEL
ENGINE**

James W. Hudson
Lieutenant, United States Navy
B.S., United States Naval Academy, 1990

Submitted in partial fulfillment of the
requirements for the degree of

MASTER OF SCIENCE IN MECHANICAL ENGINEERING

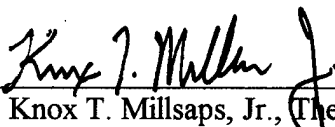
from the

NAVAL POSTGRADUATE SCHOOL
December, 1997

Author:


James W. Hudson

Approved by:


Knox T. Millsaps, Jr., Thesis Advisor


Terry R. McNelley, Chairman
Department of Mechanical Engineering

ABSTRACT

An experimental and analytical investigation was conducted to develop a calibrated torsional model of a three-cylinder, two-stroke diesel engine. A Detroit Diesel 3-53 engine was instrumented for time resolved measurement of cylinder firing pressures and high resolution near instantaneous shaft speed using a 720 and a 3,600 count per revolution optical encoder. Data were taken for three speeds and three torques for a total of nine conditions. A six degree-of-freedom torsional vibration model of the crankshaft, connecting rods, and pistons was developed. The nonlinear inertias, due to the reciprocating pistons, were included along with linear stiffness and damping. The equations of motion were numerically integrated over a cycle to obtain predicted response. The predicted response was compared to the measured response at the free end of the crankshaft.

TABLE OF CONTENTS

I.	INTRODUCTION.....	1
A.	MOTIVATION.....	1
B.	STATE OF THE ART.....	2
C.	METHODOLOGY AND OBJECTIVES.....	4
D.	ORGANIZATION.....	5
II.	TORSIONAL VIBRATION MODEL.....	7
A.	PHYSICAL SYSTEM.....	7
1.	Model Development.....	10
2.	Data Required For Model.....	11
B.	EQUATIONS OF MOTION.....	12
C.	NUMERICAL SOLUTION OF EQUATIONS OF MOTION.....	15
III.	EXPERIMENTAL SETUP.....	17
A.	THE THREE CYLINDER TWO STROKE DIESEL ENGINE.....	17
1.	Operating Conditions and Design Specifications.....	17
2.	Engine Event Timing.....	18
B.	INSTRUMENTATION.....	19
1.	Optical Encoder and Mount.....	19
2.	Pressure Transducers.....	20
3.	Modulation Domain Analyzer.....	21
4.	Data Acquisition Procedure.....	22
C.	ENGINE CYCLE ANALYZER.....	23
IV.	RESULTS.....	25
A.	MEASURED SHAFT SPEED VARIATIONS.....	25
B.	TORSIONAL VIBRATION MODEL PREDICTED RESULTS.....	28
C.	COMPARISON OF PREDICTED TO MEASURED RESPONSE.....	29
V.	CONCLUSIONS AND RECOMMENDATIONS.....	33
A.	SUMMARY.....	33
B.	CONCLUSIONS.....	33
C.	RECOMMENDATIONS.....	34
APPENDIX A	INERTIA AND STIFFNESS FOR THE TORSIONAL ENGINE MODEL.....	35
APPENDIX B	OPTICAL ENCODER AND OPTICAL ENCODER MOUNT INSTALLATION PROCEDURE.....	39
APPENDIX C	ESTABLISHING REFERENCE PRESSURE.....	41
APPENDIX D	MODULATION DOMAIN ANALYZER OPERATING PROCEDURE.....	43
APPENDIX E	DATA ACQUISITION PROCEDURE.....	47
APPENDIX F	ESTABLISHING TOP DEAD CENTER RELATIVE TO THE OPTICAL ENCODER.....	49
APPENDIX G	MATLAB CODE USED FOR CYCLE ANALYSIS.....	51
LIST OF REFERENCES.....		57
INITIAL DISTRIBUTION LIST.....		59

LIST OF FIGURES

Figure 2.1	Detroit Diesel 3-53 Engine.....	7
Figure 2.2	Relationship Between Gas Pressure Forces and Torque.....	8
Figure 2.3	Crankshaft with a Single Reciprocating Component.....	9
Figure 2.4	Torsional Vibration Model of Crankshaft.....	10
Figure 2.5	Individual Cylinder Gas Torque Contribution.....	15
Figure 3.1	Engine Event Timing Map.....	18
Figure 3.2	New Optical Encoder Mount.....	20
Figure 3.3	Reference Pressure Versus Speed Curve.....	21
Figure 3.4	Test Engine and Instrumentation.....	23
Figure 4.1	MDA Phase Lock, Ensemble Average of Raw Data.....	26
Figure 4.2	Measured Response of Crankshaft at Free End.....	28
Figure 4.3	Model Predicted Response of Crankshaft at Free End.....	29
Figure 4.4	Measured and Predicted Response of Crankshaft at Free End.....	30
Figure C.1	Instrumentation Utilized for Establishing Reference Air Box Pressure.....	42
Figure D.1	Modulation Domain Analyzer and Data Acquisition Computer.....	45
Figure E.1	Engine Cycle Analyzer, Sensor Interface, and SF-901 Computer.....	48
Figure E.2	SuperFlow Dynamometer Control Console.....	48
Figure F.1	Flywheel Access Cover.....	50

LIST OF TABLES

Table 2.1	Inertia and Stiffness of the Model.....	11
Table 3.1	Engine Characteristics.....	17
Table 4.1	Data Runs.....	25

NOMENCLATURE

η_m	Mechanical efficiency (dimensionless)
π	Pi constant
θ	Angular position of crankshaft (rads)
$\dot{\theta}$	Angular velocity of crankshaft (rad/sec)
$\ddot{\theta}$	Angular acceleration of crankshaft (rad/sec ²)
ω_{cycle}	Average angular velocity of crankshaft (rad/sec)
A_p	Cross-sectional area of piston (in ²)
C	Equivalent damping (lbf-in-sec/rad)
Δt	Measured time between successive windows of optical encoder (seconds)
F	Gas force on piston (lbf)
J	Equivalent polar moment of inertia (lbf-in-sec ²)
J_{rec}	Reciprocating inertia (lbf-in-sec ²)
K	Equivalent torsional stiffness (lbf-in/rad)
L	Length of connecting rod (in)
$P_{cyl}(t)$	Measured cylinder pressure as a function of time (psia)
R	Crankthrow eccentricity (in)
t	Time (seconds)
$T_{cyl}(t)$	Gas torque as a function of time (in-lbf)
T_{load}	Torque of the load (in-lbf)

I. INTRODUCTION

A. MOTIVATION

Diesel engines are widely used in both military and civilian applications. In the Navy, they are utilized for main propulsion and electric power generation. The reliable detection of faults both non-obtrusively and inexpensively could shift the focus of maintenance from regularly scheduled to condition based. This maintenance strategy has the potential to save costly, unneeded maintenance and can increase availability of diesel engines.

Individual cylinder pressures of internal combustion engines are excellent predictors of many types of engine faults. Cylinder pressures are directly related to the torque output capability of an engine. Therefore, the contribution of torque from an individual cylinder is directly related to the maximum pressure that cylinder develops. Cylinders experiencing loss of pressure can be caused by faulty fuel injectors, worn cylinder lining, faulty piston rings, leaking valves, and blown or leaking cylinder head gaskets.

There is a problem with measuring cylinder firing pressures in the field. While high quality pressure transducers can accurately measure cylinder pressures, they have a limited lifetime in the combustion chamber environment and are expensive. Many alternative indirect methods of cylinder pressure monitoring such as the use of strain bolts are being explored.

Another indirect method is to measure the variations in shaft speed. With this information and equations of motion describing the dynamics of the engine, the firing pressures are solved for numerically. In order to accurately predict cylinder firing pressures with shaft speed variation, an accurate torsional engine model representative of the physical system is required.

B. STATE OF THE ART

There have been numerous research efforts focused on extracting cylinder pressure information from crankshaft speed fluctuations. It is well known that these speed fluctuations are a direct result of the cyclic nature of the crankshaft torque waveform. This torque waveform is a direct result from gas pressure forces, due to combustion, and inertia forces, due to internal reciprocating masses. The challenge has been taking these measured speed fluctuations and passing them through a robust engine model to predict cylinder pressures. This literature review focused in areas of non-obtrusive cylinder pressure and torque prediction with emphasis on torsional vibration modeling.

Wilson [Ref. 1] developed a torsional vibration model of a crankshaft with reciprocating components. With his methods, the individual inertia, stiffness, and damping between cylinder crankthrows and the rest of the shaft are readily determined. His methods are currently used by industry to develop torsional vibration models of crankshafts. Kabele [Ref. 2] developed a torsional vibration model of a diesel crankshaft which included piston and ring friction, connecting rod plane motion, hysteretic damping in the crankshaft, and cylinder pressure as a forcing function. The model was derived

from Newtonian Mechanics and the governing differential equations were non-linear making a numerical solution necessary. Once his model was developed, he compared measured and model predicted vibration amplitudes for various harmonic orders and concluded that correlation between the two was excellent. The measured vibration amplitudes were from a V-8 diesel engine.

Citron et al, [Ref 3] did a computer simulation and produced cylinder pressure torque waveforms by using an elastic model of an engine, drivetrain system, and measured speed fluctuations. These speed fluctuation data were passed back through the model to determine the fluctuation waveform of both the total engine torque being developed and the cylinder pressure waveform which gave rise to it.

Rizzoni [Ref. 4] proposed passing crankshaft speed fluctuations through an equivalent electronic circuit representing engine dynamics to predict cylinder misfires. He conducted experimental work on production spark ignited vehicles and confirmed that it is possible to apply this method with minimal hardware and computational overhead.

Sobel et al, [Ref. 5] described a technique for measuring instantaneous crankshaft torque utilizing a non-contact ferromagnetic material to measure torsional stress in the crankshaft. The instantaneous torque of an internal combustion, four-cylinder engine was measured at the flywheel and compared with pressure signals during bench tests. Excellent correlation between this non-contact measured torque and values of the mean effective pressure for each cylinder were obtained.

Brown and Neill [Ref 6] presented a non-contact method for determining simultaneously the pressure in each cylinder by employing a pattern recognition technique

to compare crankshaft speed fluctuations to reference patterns in a knowledge base. The non-contact method utilized was an interval timer and a magnetic sensor which timed the flywheel gear teeth as they passed. The experiment was carried out on a Detroit Diesel 6V-92TA engine. The experimental results show that the method evaluates the cylinder pressures with an RMS error of less than six percent. But this requires extensive data bases for each condition.

Bell [Ref. 7] concluded, utilizing the same Detroit Diesel 3-53 engine used in this research, that the variation of shaft speed held information which could be used to predict cylinder firing pressures. He also recommended the development of a torsional vibration model of the engine and flywheel system along with a more rigid optical encoder mounting for more accurate time resolved measurement.

C. METHODOLOGY AND OBJECTIVES

The engine used for this research is a Detroit Diesel Series 53 engine, model 5033-5001N. It is a three-cylinder, two-stroke engine. During one revolution, the crankshaft speed fluctuates as a result of cylinder pressure variations. These crankshaft speed fluctuations can be measured using an optical encoder. A torsional vibration model with nonlinear inertias, due to the reciprocating pistons, and linear stiffness and damping will be developed to represent the dynamics of the engine. The torsional vibration model will be calibrated by ensuring, as closely as possible, predicted response matches the measured response. Data from these measured speed fluctuations can then later be passed through the calibrated torsional model to determine cylinder firing pressures

The objectives of this thesis are to:

1. Instrument a diesel engine with a rigid optical encoder mount such that reliable time resolved measurements of crankshaft speed relative to the engine block can be obtained.
2. Develop a torsional vibration model of the crankshaft including components connected to it (i.e. connecting rods, pistons, flywheels, and external loads).
3. Operate the diesel engine at several speeds and applied torques to establish baseline data.
4. Compare the model predicted response to the experimental measured response.

D. ORGANIZATION

Chapter II describes the development of the crankshaft torsional vibration model. Equations of motion are derived for a six degree-of-freedom torsional model and numerical solution procedure is presented.

Chapter III describes the engine, dynamometer, instrumentation, and data acquisition procedures.

Chapter IV presents results of data acquisition, the measured response, and the model predicted response. A comparison of measured to predicted response is made based on the results.

Chapter V contains summary, conclusions, and recommendations for future work.

II. TORSIONAL VIBRATION MODEL

A. PHYSICAL SYSTEM

The engine used for this research is representative of diesel engines. It is a three-cylinder, two-stroke engine. Engine operating conditions and design specifications are discussed in more detail in Section III. A.

Figure 2.1 illustrates the engine layout with the crankshaft, flywheel, pistons and connecting rods. The front of the engine is to the left. The cylinders are numbered from front (1) to back (3). Connected to the power take-off shaft on the right is the load, which in this case is supplied by a water brake dynamometer. The firing order is 1-3-2 and the crankshaft rotates clockwise as seen from the front.

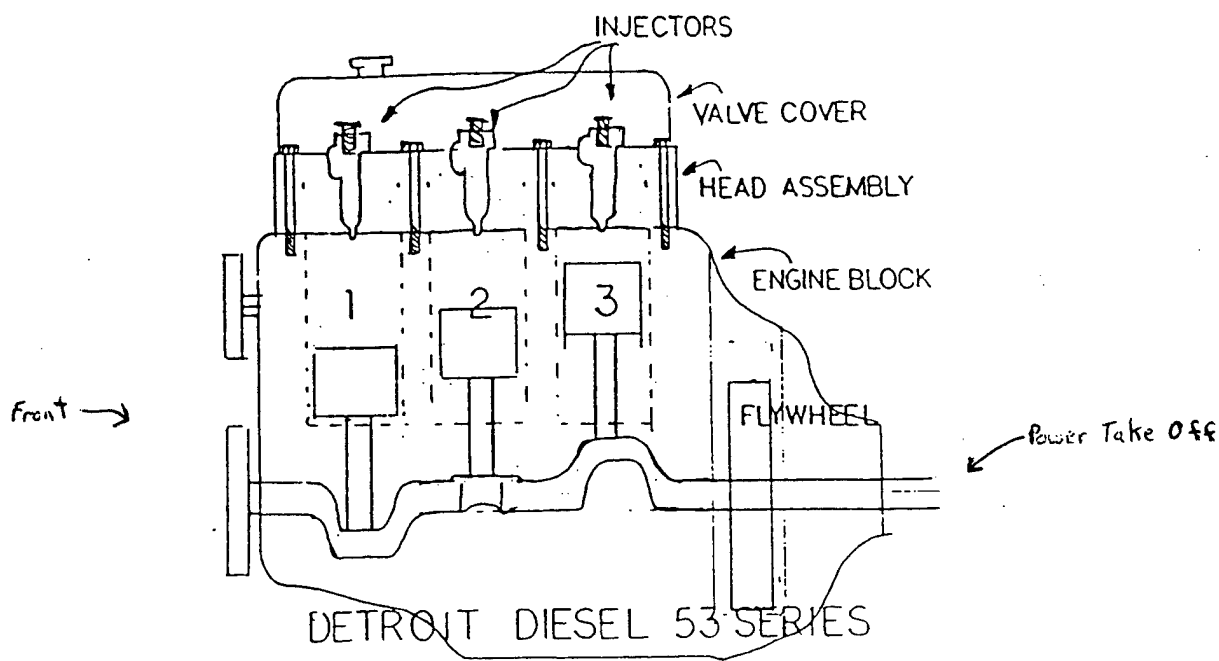
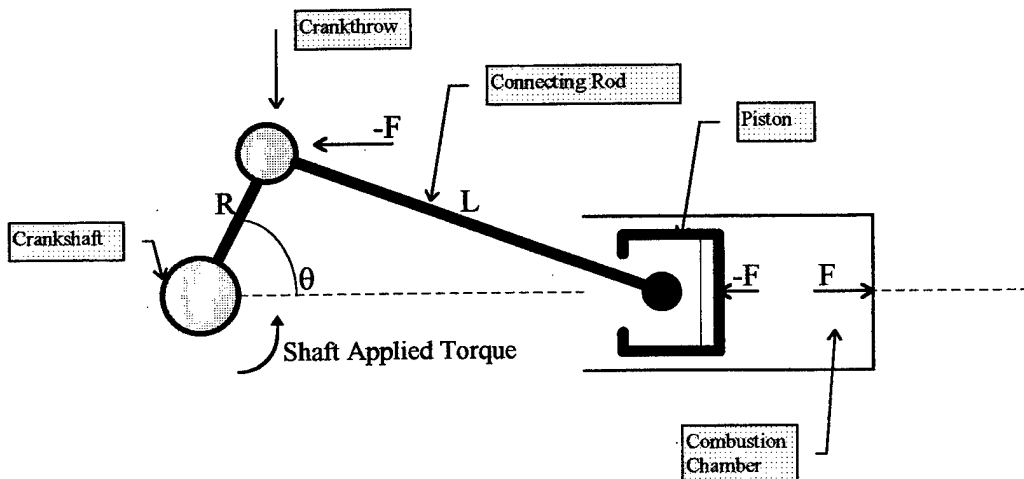


Figure 2.1 Detroit Diesel 3-53 with crankshaft and major reciprocating components. The front of the engine is the left hand side.

The crankshaft crankthrows are the locations where the connecting rods are attached to the crankshaft. Crankthrows number one, two, and three are displaced 120 degrees. After the number one piston reaches top dead center (TDC), its highest point of travel, 120 degrees of crankshaft rotation later the number three piston arrives at its TDC. Number two piston's TDC is 240 degrees after number one. The power into the crankshaft is delivered at each crankthrow.

The forces due to gas pressure in each cylinder can be taken as a force ' $-F$ ' on the piston and an equal and opposite force ' F ' on the cylinder head. The force ' $-F$ ' is transmitted through the connecting rod to the crankthrow. The resultant force on the crankshaft multiplied by the eccentricity ' R ' of the crankthrow creates the gas torque. If there were no friction, the gas torque would equal the shaft applied torque. Figure 2.2 shows the relationship between gas pressure force and torque.



where:
 F = cylinder pressure * area of the piston (lbf)
 R = crankthrow eccentricity (in)
 $θ$ = angular position of crankshaft relative to TDC (rad)
 L = length of connecting rod (in)

Figure 2.2 Relationship between gas pressure forces and gas torque into the crankshaft.

Gas torque into the crankshaft as a result of cylinder gas pressures is given by the following relationship:

$$\begin{aligned}
 T_{1\text{cyl}} &= P_{1\text{cyl}} R \sin(\theta) A_p & \text{where: } P_{\# \text{cyl}} &= \text{Measured cylinder pressure (psia)} \\
 T_{2\text{cyl}} &= P_{2\text{cyl}} R \sin(\theta - 4\pi/3) A_p & R &= \text{Crankshaft crankthrow eccentricity (in)} \\
 T_{3\text{cyl}} &= P_{3\text{cyl}} R \sin(\theta - 2\pi/3) A_p & \theta &= \text{Angular position of #1 crankthrow} \\
 & & & \text{after TDC (rad)} \\
 (2.1) & & A_p &= \text{Cross-sectional area of the pistons (in}^2\text{)}
 \end{aligned}$$

The torque applied to the crankshaft is somewhat less than the gas torques due mainly to friction on the cylinder wall (rings). The major components considered in the development of a torsional vibration model are the crankshaft, pistons, connecting rods, and flywheel. This physical system to be modeled is shown in Figure 2.3.

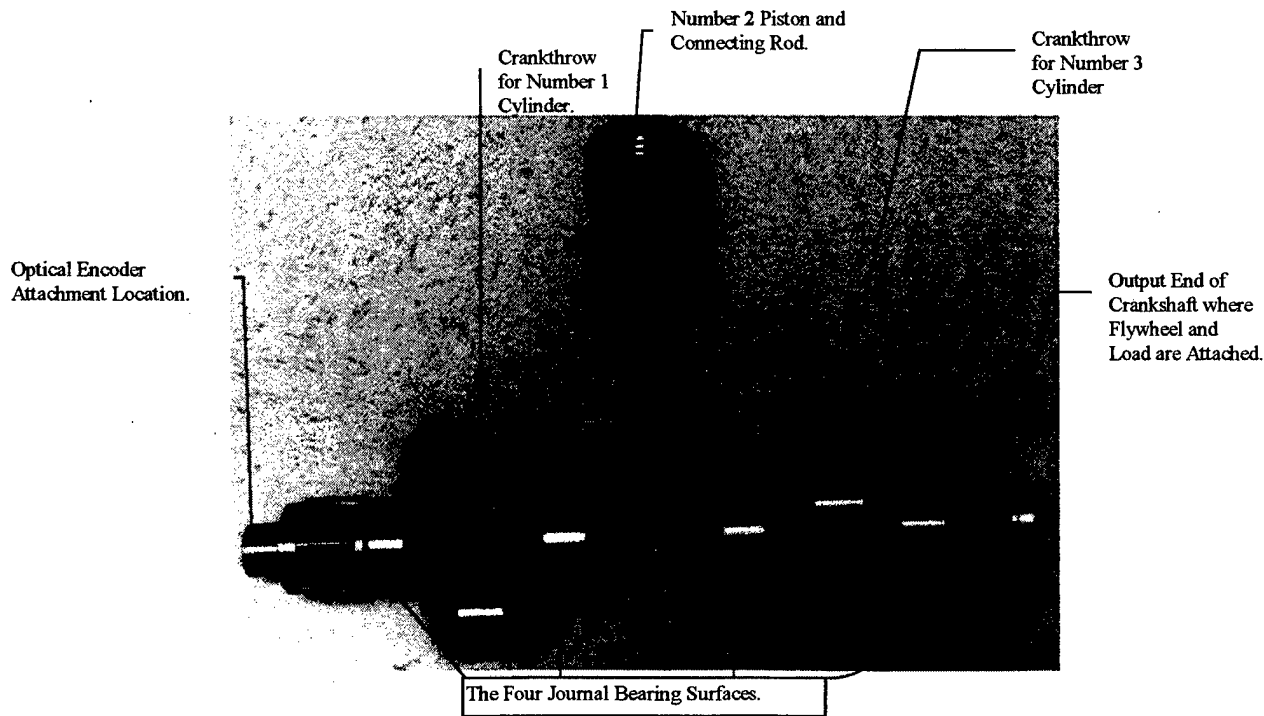


Figure 2.3 Crankshaft with a single reciprocating component.

1. Model Development

The reciprocating components of the engine are very complex. However, to facilitate calculation it is useful to represent the complex system by a reduced order system. For this research, six rigid masses connected by sections of shafting with torsional stiffness and damping shall be used. This reduced system should retain the dominant dynamic characteristics of the original physical system that are of interest. The six degree-of-freedom torsional vibration model that is used to represent the physical system is shown in Figure 2.4.

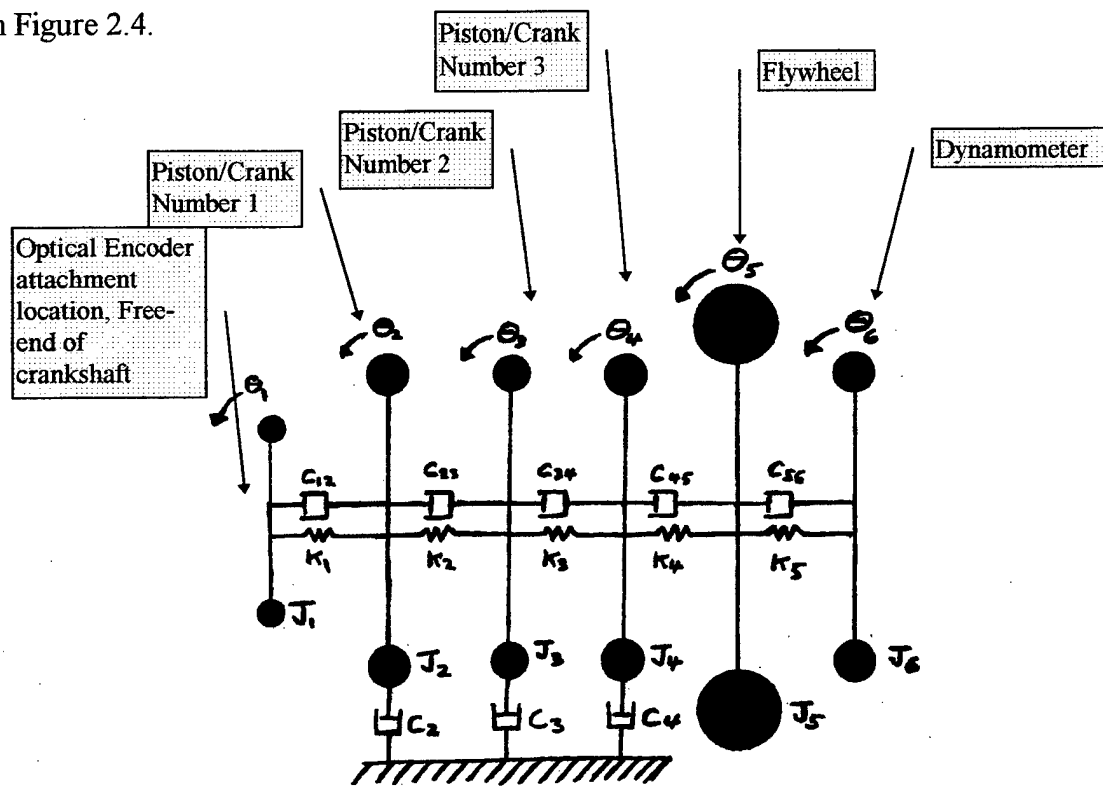


Figure 2.4 Torsional vibration model of crankshaft and reciprocating components.

In Figure 2.4, θ_1 represents the angular position of the crankshaft where the optical encoder attaches, θ_2 through θ_4 represents the angular position of crankthrows number one through three, θ_5 represents the angular position of the flywheel, and θ_6 represents the

angular position of the load (water brake dynamometer). Each 'J' represents the equivalent mass polar moment of inertia at each degree of freedom. Equivalent torsional stiffness between each degree of freedom is represented by K_1 through K_5 . The material damping of the crankshaft between each degree of freedom is represented by C_{12} , C_{23} , C_{34} , C_{45} , and C_{56} . The linear viscous damping effects of each cylinder due to translation of the pistons in the cylinders and oil at the journal bearing surfaces are represented by C_2 , C_3 , and C_4 . All inertias (J's) and stiffnesses (K's) are readily determined by the geometry and material properties of the system. Procedures for determining the equivalent inertia and stiffness for the model are outlined in Appendix A. The damping for the system, especially viscous damping effects, are not so readily determined and will be discussed later when comparing measured results to model predicted results. Table 2.1 defines the values of inertia (J's) and stiffness (K's) for the model [Ref. 8].

Table 2.1 Inertia and Stiffness of the model.

INERTIA	STIFFNESS
$J_1 = 0.029 \text{ lb}_f\text{-in}\cdot\text{sec}^2$	$K_1 = 3.470 \times 10^6 \text{ lb}_f\text{-in/rad}$
$J_2 = 0.273 + 0.069[1-\cos(2\theta)] \text{ lb}_f\text{-in}\cdot\text{sec}^2$	$K_2 = 9.551 \times 10^6 \text{ lb}_f\text{-in/rad}$
$J_3 = 0.171 + 0.069[1-\cos2(\theta-2\pi/3)] \text{ lb}_f\text{-in}\cdot\text{sec}^2$	$K_3 = 9.551 \times 10^6 \text{ lb}_f\text{-in/rad}$
$J_4 = 0.273 + 0.069[1-\cos2(\theta-4\pi/3)] \text{ lb}_f\text{-in}\cdot\text{sec}^2$	$K_4 = 13.49 \times 10^6 \text{ lb}_f\text{-in/rad}$
$J_5 = 6.194 \text{ lb}_f\text{-in}\cdot\text{sec}^2$	$K_5 = 1.304 \times 10^6 \text{ lb}_f\text{-in/rad}$
$J_6 = 0.280 \text{ lb}_f\text{-in}\cdot\text{sec}^2$	

2. Data Required For Model

Physical dimensions were obtained by measuring the geometry of an equivalent crankshaft out of an engine of the same model as shown in Figure 2.3. The material used to manufacture the crankshaft is Steel SAE 1548 Modified (Maganese 1.00/1.30 and

Carbon 0.43/0.52). Both the physical dimensions and material properties were checked against the manufacturer's design drawings [Ref. 9]

Other data required for the model are measured gas torque as a function of angular position and load torque

B. EQUATIONS OF MOTION

Referring to Figure 2.4, the equations governing the motion of the system are:

- (1) $J_1\ddot{\theta}_1 + C_{12}(\dot{\theta}_1 - \dot{\theta}_2) + K_1(\theta_1 - \theta_2) = 0$
- (2) $(J_2 + J_{2rec})\ddot{\theta}_2 + C_{12}(\dot{\theta}_2 - \dot{\theta}_1) + K_1(\theta_2 - \theta_1) + C_{23}(\dot{\theta}_2 - \dot{\theta}_3) + K_2(\theta_2 - \theta_3) + C_2\dot{\theta}_2 = T_{1cyl}(t)$
- (3) $(J_3 + J_{3rec})\ddot{\theta}_3 + C_{23}(\dot{\theta}_3 - \dot{\theta}_2) + K_2(\theta_3 - \theta_2) + C_{34}(\dot{\theta}_3 - \dot{\theta}_4) + K_3(\theta_3 - \theta_4) + C_3\dot{\theta}_3 = T_{2cyl}(t)$
- (4) $(J_4 + J_{4rec})\ddot{\theta}_4 + C_{34}(\dot{\theta}_4 - \dot{\theta}_3) + K_3(\theta_4 - \theta_3) + C_{45}(\dot{\theta}_4 - \dot{\theta}_5) + K_4(\theta_4 - \theta_5) + C_4\dot{\theta}_4 = T_{3cyl}(t)$
- (5) $J_5\ddot{\theta}_5 + C_{45}(\dot{\theta}_5 - \dot{\theta}_4) + K_4(\theta_5 - \theta_4) + C_{56}(\dot{\theta}_5 - \dot{\theta}_6) + K_5(\theta_5 - \theta_6) = 0$
- (6) $J_6\ddot{\theta}_6 + C_{56}(\dot{\theta}_6 - \dot{\theta}_5) + K_5(\theta_6 - \theta_5) = -T_{load}$

(2.2)

The equations of motion in matrix format are:

$$\begin{bmatrix} J_1 & 0 & 0 & 0 & 0 & 0 \\ 0 & J_2 + J_{2rec} & 0 & 0 & 0 & 0 \\ 0 & 0 & J_3 + J_{3rec} & 0 & 0 & 0 \\ 0 & 0 & 0 & J_4 + J_{4rec} & 0 & 0 \\ 0 & 0 & 0 & 0 & J_5 & 0 \\ 0 & 0 & 0 & 0 & 0 & J_6 \end{bmatrix} \begin{Bmatrix} \ddot{\theta}_1 \\ \ddot{\theta}_2 \\ \ddot{\theta}_3 \\ \ddot{\theta}_4 \\ \ddot{\theta}_5 \\ \ddot{\theta}_6 \end{Bmatrix} +$$

$$\begin{bmatrix} C_{12} & -C_{12} & 0 & 0 & 0 & 0 \\ -C_{12} & C_{12} + C_{23} + C_2 & -C_{23} & 0 & 0 & 0 \\ 0 & -C_{23} & C_{23} + C_{34} + C_3 & -C_{34} & 0 & 0 \\ 0 & 0 & -C_{34} & C_{34} + C_{45} + C_4 & -C_{45} & 0 \\ 0 & 0 & 0 & -C_{45} & C_{45} + C_{56} & -C_{56} \\ 0 & 0 & 0 & 0 & -C_{56} & C_{56} \end{bmatrix} \begin{bmatrix} \dot{\theta}_1 \\ \dot{\theta}_2 \\ \dot{\theta}_3 \\ \dot{\theta}_4 \\ \dot{\theta}_5 \\ \dot{\theta}_6 \end{bmatrix} +$$

$$\begin{bmatrix} K_1 & -K_1 & 0 & 0 & 0 & 0 \\ -K_1 & K_1 + K_2 & -K_2 & 0 & 0 & 0 \\ 0 & -K_2 & K_2 + K_3 & -K_3 & 0 & 0 \\ 0 & 0 & -K_3 & K_3 + K_4 & -K_4 & 0 \\ 0 & 0 & 0 & -K_4 & K_4 + K_5 & -K_5 \\ 0 & 0 & 0 & 0 & -K_5 & K_5 \end{bmatrix} \begin{bmatrix} \theta_1 \\ \theta_2 \\ \theta_3 \\ \theta_4 \\ \theta_5 \\ \theta_6 \end{bmatrix} = \begin{bmatrix} 0 \\ T_{1cyl}(t) \\ T_{2cyl}(t) \\ T_{3cyl}(t) \\ 0 \\ -T_{Load} \end{bmatrix}$$

(2.3)

The reciprocating component of inertia at each crankthrow, J_{2rec} , J_{3rec} , and J_{4rec} , represent the inertia contribution of the piston and connecting rod. The influence of these reciprocating components is a maximum when the crankshaft is at the position corresponding to mid-stroke (90 degrees after top dead center), and disappears when the crank is on top or bottom dead center (0 or 180 degrees after top dead center). The relationship of the non-linear reciprocating inertia to crankshaft position is:

$$\begin{aligned} J_{2rec} &= WR^2/2g[1-\cos(2\theta)] & \text{where: } W = \text{Weight of piston and connecting rod (10.5 lbf)} \\ J_{3rec} &= WR^2/2g[1-\cos(2(\theta-2\pi/3))] & R = \text{Crankshaft crankthrow eccentricity (2.25 in)} \\ J_{4rec} &= WR^2/2g[1-\cos(2(\theta-4\pi/3))] & g = \text{Acceleration of gravity (386 in/sec}^2\text{)} \\ & & \theta = \text{Angular position of #1 crankthrow after} \\ & & \text{TDC (rad)} \end{aligned} \quad (2.4)$$

The right hand side of the equations of motion are the applied torques [$T_{1cyl}(t)$, $T_{2cyl}(t)$, and $T_{3cyl}(t)$] into the system and load torque, T_{load} (which is considered constant), out of the system. Figure 2.5 shows an example of individual measured cylinder gas torque contribution referenced to top dead center of number one cylinder. Since the total gas torque into the system has to overcome damping and friction before it exits as useful torque (load torque), the gas torques can be multiplied by some factor to account for the losses. It is also possible to subtract a constant parasitic torque from each cylinder gas torque. Integrating each cylinder torque curve with respect to angular position yields an average torque. Dividing the load torque by the sum of the three average cylinder torques will yield the mechanical efficiency (η_m) to be used. Specifically:

$$\bar{T}_{in} = \frac{1}{2\pi} \int_0^{2\pi} T(t) d\theta \quad \text{and} \quad \eta_m = \frac{T_{out}}{\bar{T}_1 + \bar{T}_2 + \bar{T}_3} \quad (2.5)$$

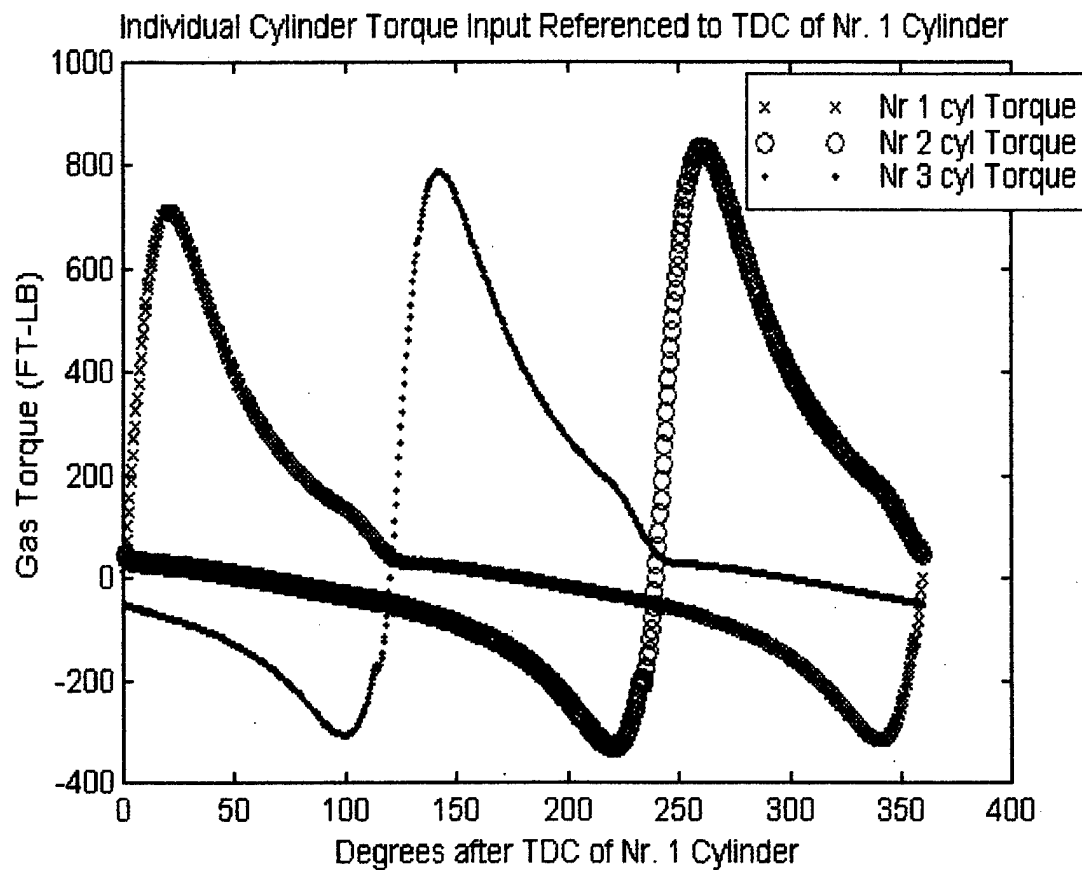


Figure 2.5 Individual cylinder gas torque contribution referenced to Nr. 1 cylinder top dead center (TDC).

C. NUMERICAL SOLUTION OF EQUATIONS OF MOTION

In order to solve the six second order equations of motion it is first necessary to reduce them to a system of twelve first order differential equations. These are:

$$\begin{aligned}
\theta_7 &= \dot{\theta}_1 \\
\theta_8 &= \dot{\theta}_2 \\
\theta_9 &= \dot{\theta}_3 \\
\theta_{10} &= \dot{\theta}_4 \\
\theta_{11} &= \dot{\theta}_5 \\
\theta_{12} &= \dot{\theta}_6 \\
J_1 \dot{\theta}_7 - C_{12} \theta_8 + C_{12} \theta_7 - K_1 \theta_2 + K_1 \theta_1 &= 0 \\
(J_2 + J_{2rec}) \dot{\theta}_8 - C_{23} \theta_9 + (C_{23} + C_{12} + C_2) \theta_8 - C_{12} \theta_7 - K_2 \theta_3 + (K_1 + K_2) \theta_2 - K_1 \theta_1 &= T_{1cyl}(t) \\
(J_3 + J_{3rec}) \dot{\theta}_9 - C_{34} \theta_{10} + (C_{34} + C_{23} + C_3) \theta_9 - C_{23} \theta_8 - K_3 \theta_4 + (K_2 + K_3) \theta_3 - K_2 \theta_2 &= T_{2cyl}(t) \\
(J_4 + J_{4rec}) \dot{\theta}_{10} - C_{45} \theta_{11} + (C_{45} + C_{34} + C_4) \theta_{10} - C_{34} \theta_9 - K_4 \theta_5 + (K_3 + K_4) \theta_4 - K_3 \theta_3 &= T_{3cyl}(t) \\
J_5 \dot{\theta}_{11} - C_{56} \theta_{12} + (C_{56} + C_{45}) \theta_{11} - C_{45} \theta_{10} - K_5 \theta_6 + (K_4 + K_5) \theta_5 - K_4 \theta_4 &= 0 \\
J_6 \dot{\theta}_{12} + C_{56} \theta_{12} - C_{56} \theta_{11} + K_5 \theta_6 - K_5 \theta_5 &= -T_{load}
\end{aligned} \tag{2.6}$$

This initial value problem was solved using a fourth order Runge-Kutta method ordinary differential equation solver (ODE45 in MATLAB). Twelve initial conditions are required, namely, angular position $\theta(t = 0)$ and angular velocity $\dot{\theta}(t = 0)$. The system repeats after one revolution of the crankshaft (2π rad). A numerical solution for the predicted angular position of the first degree of freedom is calculated and presented in Section IV. B.

III. EXPERIMENTAL SETUP

A. THE THREE CYLINDER TWO STROKE DIESEL ENGINE

1. Operating Conditions and Design Specifications

The test engine used is a Detroit Diesel Series 53 two stroke three cylinder engine.

The engine design operating characteristics are listed in Table 3.1.

Table 3.1 Engine Characteristics [Ref. 10]

Model	5033-5001N
Engine Type	In line-2 Cycle-Naturally Aspirated
Number of Cylinders	3
Bore and Stroke	3.875 x 4.50 inches
Exhaust Valves per cylinder	4
Engine Displacement	159 cubic inches
Compression Ratio	21.0:1
Maximum Power Output	92 bhp
Full Load Speed	2,800 RPM
Peak Torque	198 ft-lbs
Peak Torque Speed	1,500 RPM
Brake Mean Effective Pressure	83 $\frac{lb}{in^2}$

The manufacturer provides the following estimate of cylinder combustion pressures based upon an empirically obtained relationship:

$$C_p = \frac{4,650,000 \cdot IHP}{B^2 S \cdot N \cdot RPM} \text{ where: } C_p = \text{Combustion pressure (psia)}, \quad (3.1)$$

N = No. of cylinders

B = Bore (in), S = Stroke (in),

IHP = indicated horsepower ($\frac{BHP}{IHP} = \eta_{mech} \approx 0.70$)

RPM = revolutions per minute of crankshaft.

This formula gives values within $\pm 5\%$ for speeds (1200 RPM to maximum rated RPM) and power (continuous to maximum intermittent rated power). [Ref. 11] Appendix B [Ref. 12] provides rated power as a function of speed curves and engine specification data.

2. Engine Event Timing

The major events occurring in the cylinders with respect to crankshaft angle are given in Figure 3.1, specifically, intake port, exhaust valve, and fuel injector movements with respect to top dead center of the number one cylinder. The firing order of the engine (1-3-2) can clearly be seen. The number three cylinder and number one cylinder events occur 120 and 240 degrees respectively after the corresponding number one cylinder

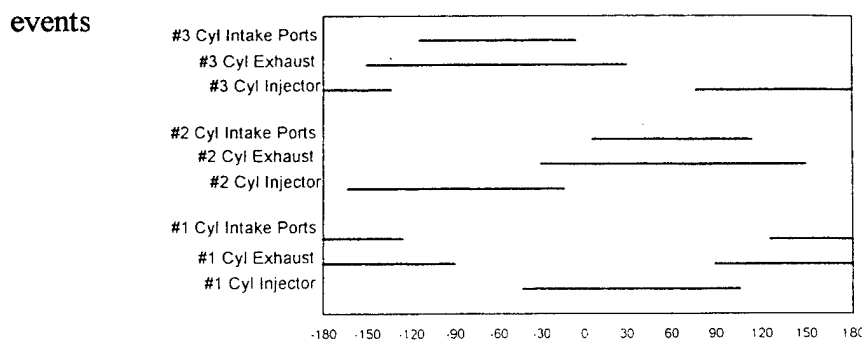


Figure 3.1 Engine event timing map referenced to TDC Nr. 1 cylinder

B INSTRUMENTATION

1. Optical Encoder and Mount

The optical encoder mount holds the casing of the optical encoder while the shaft of the encoder is connected to the crankshaft. The mount is in turn attached to the engine block. Any torsional displacement between the mount and the engine block will introduce errors and hence are to be minimized. The two previous generations of optical encoder mounts allowed the encoders to move too much during engine operation. The first encoder mount did not provide adequate support for the encoder bearings [Ref. 7] The second encoder mount was essentially an aluminum plate mounted on the end of three cantilevered beams. When a proximeter was used to measure the displacement of the aluminum plate with respect to the engine block, it was determined that the optical encoder mount was moving approximately ± 0.02 degrees with respect to the engine block across a wide variation of speeds and torques. This relative displacement, however small it seems, corresponds to a 20% error in Δ_t readings with a 3600 count optical encoder, and a 4% error in Δ_t readings from a 720 count optical encoder. These magnitudes of error are unacceptable when changes in Δ_t 's between different angular positions can vary by as little as three microseconds. A new more rigid optical encoder mount was designed and successfully installed.

Appendix B describes the design of the new optical encoder mount and optical encoder installation procedure. Appendix F is the procedure for establishing top dead center (TDC) relative to the optical encoder. All events for data collection are referenced to TDC of the number one piston. Figure 3.2 shows the new optical encoder mount.

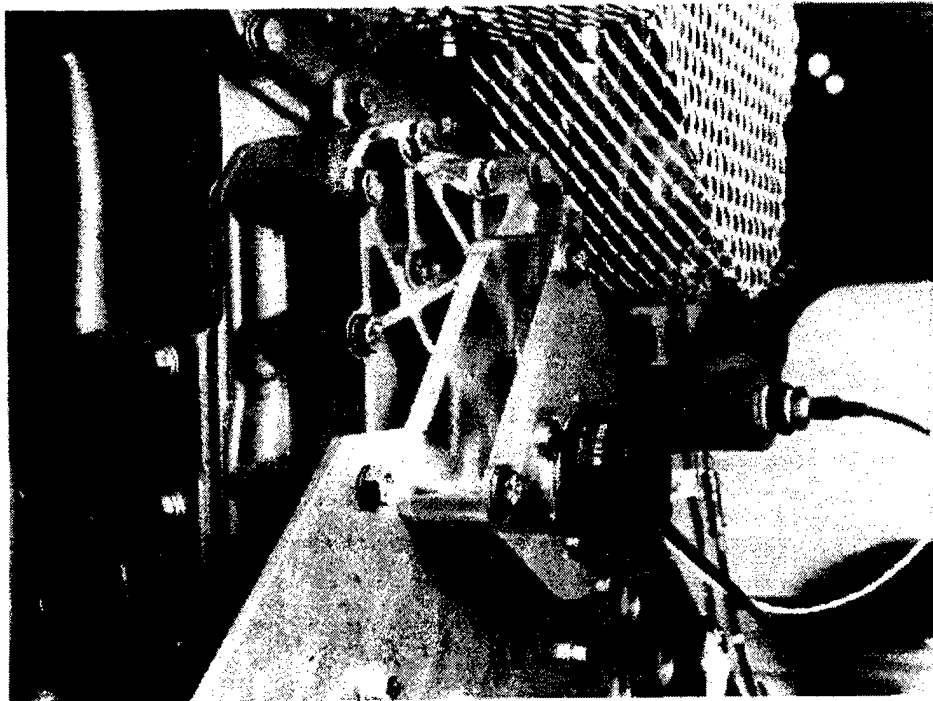


Figure 3.2 New optical encoder mount

2. Pressure Transducers

These pressure transducers are used to measure gas pressure inside the cylinders for cylinder pressure versus crank position data collection. Cylinder pressure is a necessary component in the solution of the model predicted response.

Reference air pressure is a required input for the Engine Cycle Analyzer software. These pressure transducers required a reference pressure to properly measure the absolute pressure. This reference pressure is the air box pressure or the air pressure the cylinder experiences when the intake ports are exposed (see Figure 3.1). A pressure comparator connected to the spark plug mounting hole in the side of the engine was used to establish a

reference pressure versus engine speed curve. Figure 3.3 is the measured pressure in the air box versus engine speed curve. Appendix C describes the procedure used to establish the curve.

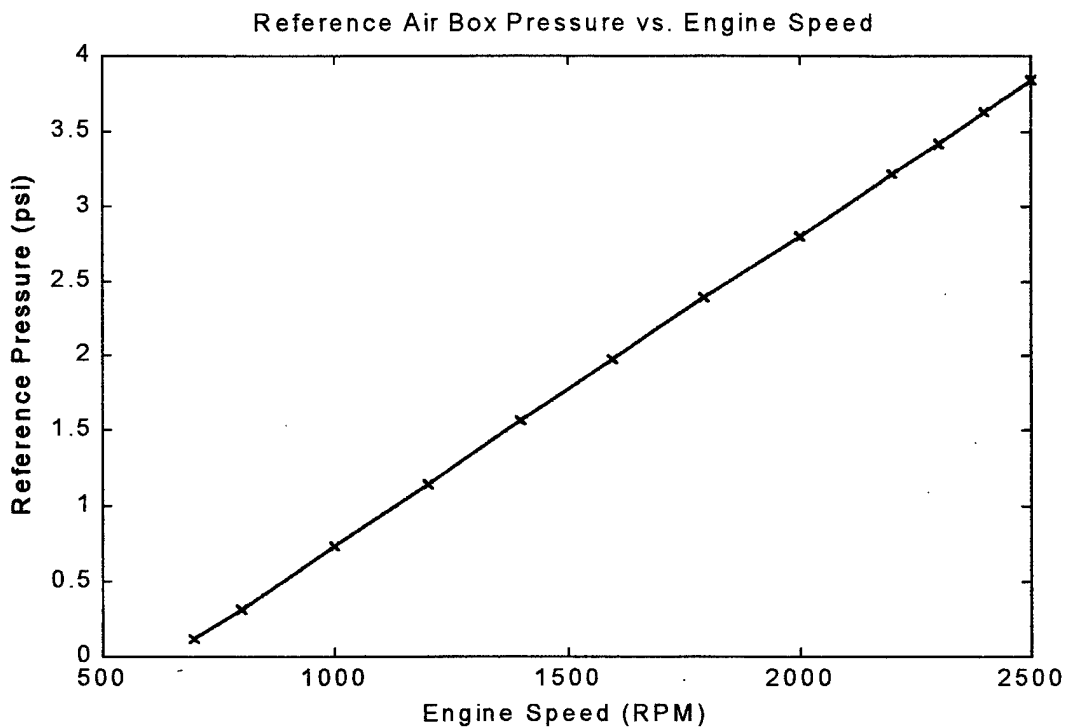


Figure 3.3. Reference pressure versus speed curve

3. Modulation Domain Analyzer

A Hewlett Packard 53310A Modulation Domain Analyzer (MDA) was used to measure the time intervals between successive windows of the optical encoder and hence determine $\theta(t)$, $\dot{\theta}(t)$, and $\ddot{\theta}(t)$. This device measures frequency or time interval (Δt) between successive events versus time (the modulation domain). The optical encoder installed on the engine provides an output signal of a repeating five volt TTL

square wave with each rise corresponding to a known angular position (0.1 degrees for a 3600 count optical encoder and 0.5 degrees for a 720 count optical encoder). With the 32,000 bit extended memory option, eight revolutions of crankshaft information using the 3,600 count optical encoder and 44 revolutions of information using the 720 count optical encoder (8 revs x 3600 events per rev = 28,800 events and 44 revs x 720 events per rev = 31,680 events) could be recorded and stored. This information is used to compare measured angular position to model predicted angular position in Section IV. C.

The procedures for measuring Δ_t 's from the optical encoder, accessing this data from the memory of the MDA, and storing it to facilitate passage to software such as MATLAB is discussed in Appendix D.

4. Data Acquisition Procedure

Figure 3.4 is a schematic of the test engine and instrumentation. Appendix E describes the data acquisition procedure.

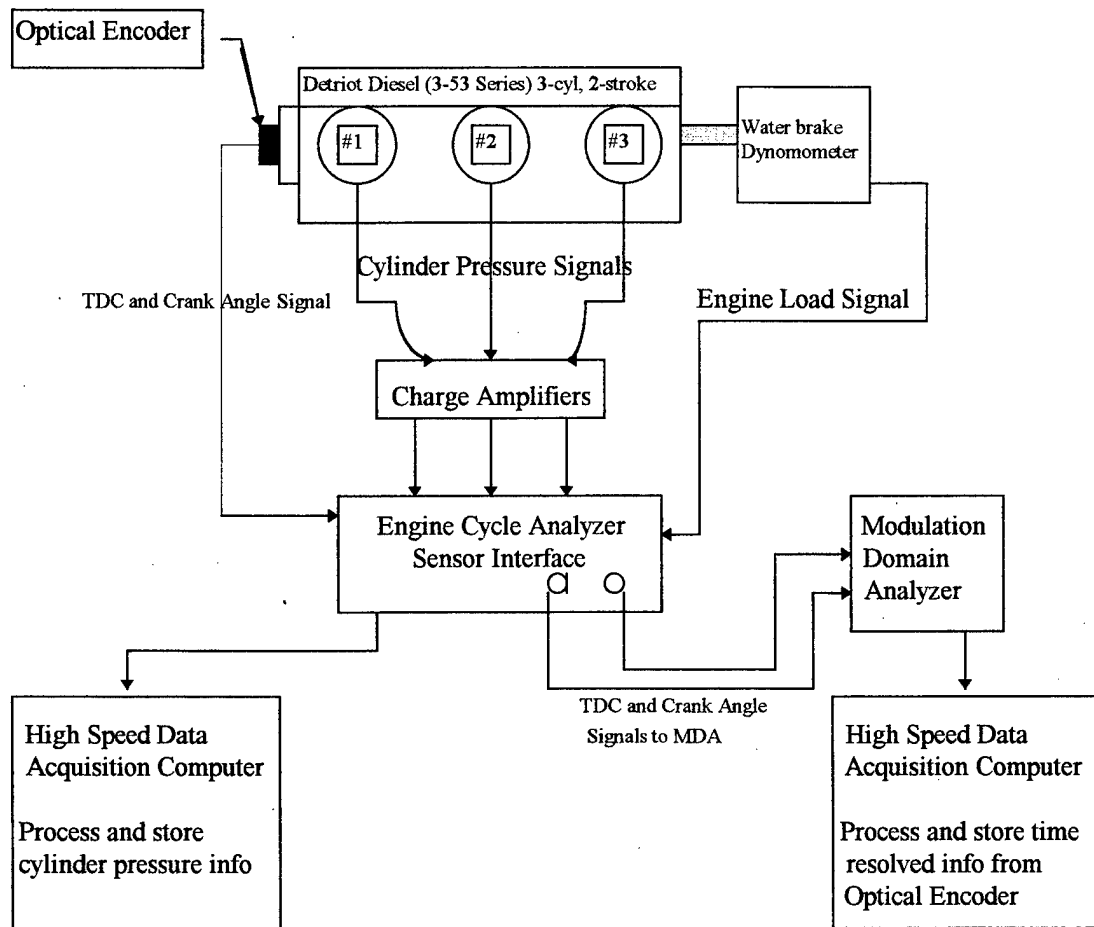


Figure 3.4 Test engine and instrumentation

C. ENGINE CYCLE ANALYZER

The Engine Cycle Analyzer (ECA) manufactured by SuperFlow is a PC based data acquisition system which allows pressure versus angular position of the crankshaft data to be measured and stored. During data acquisition, the ECA was used to record and store pressure data from all three cylinders. The ECA has the ability to monitor 1 to 999 revolutions of data from the engine and store the ensemble average of this data to memory. When using the 3,600 count optical encoder, 8 revolutions of data were recorded and when using the 720 count optical encoder, 44 revolutions of data were

recorded. These number of cycles were chosen to match the maximum number of cycles that the MDA could store. Revolutions of recorded data corresponded to the data collection capability of the MDA. Appendix E discusses operation of the ECA and setup files.

IV. RESULTS

A. MEASURED SHAFT SPEED VARIATIONS

To obtain a sufficient data base, time resolved cylinder pressures and near instantaneous shaft speed were acquired for all combination of speeds and torques shown in Table 4.1. These represent low, medium, and high torque and low, medium, and high speed. For each condition (e.g. 1,000 RPM, 135 FT-LBS) data were acquired with both the 720 count and the 3,600 count optical encoder.

Table 4.1 Data runs

SPEED (RPM)	MEASURED LOAD TORQUE (FT-LBS)		
1000	22	80	135
1500	22	135	160
2000	50	135	200

Only the result of the 1,000 rpm and 135 ft-lb run utilizing the 720 count optical encoder was chosen for analysis. Raw data from the Modulation Domain Analyzer was phase locked and ensemble averaged to represent one typical cycle (0 to 360 degrees after TDC). Appendix G is the MATLAB code which phase locks and ensemble averages the raw data. Figure 4.1 is a plot of the phase locked, ensemble average data from the MDA for 44 cycles taken at 1,000 RPM and 135 FT-LBS torque.

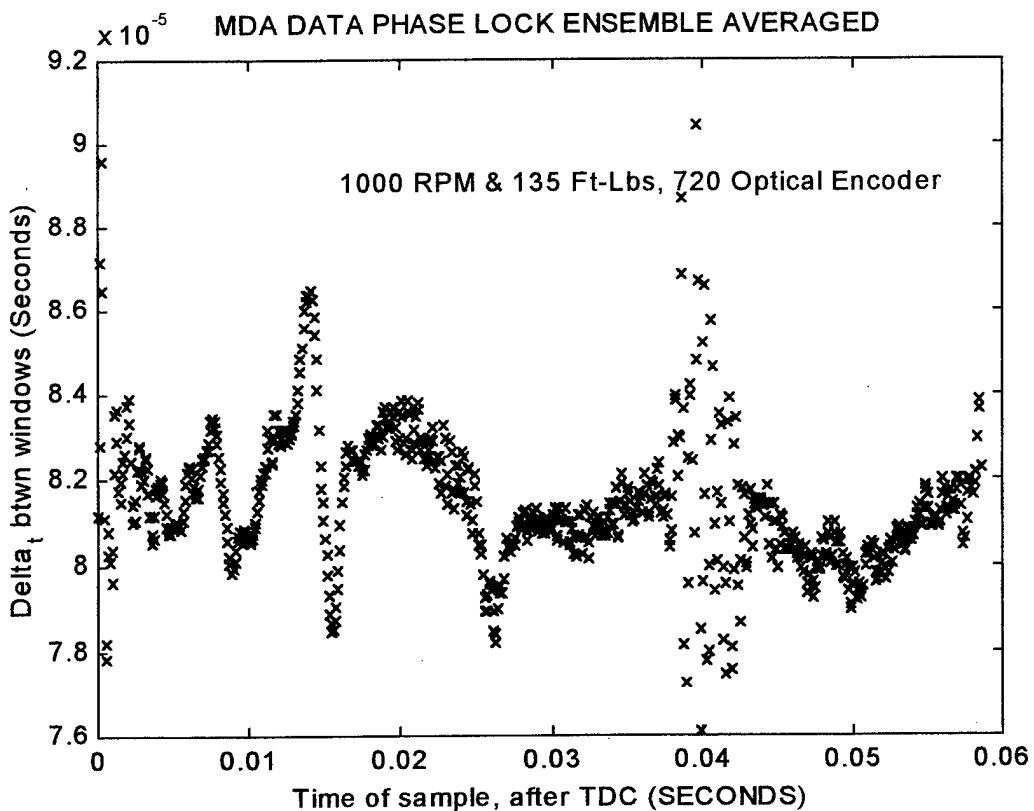


Figure 4.1 MDA phase locked, ensemble average of raw data taken at 1,000 rpm and 135 ft-lbs.

Figure 4.1 shows on the ordinate the time between successive windows (delta_t) for the optical encoder versus time. This corresponds to 360 degrees of data. If the crankshaft were turning with a constant angular velocity, the data shown in Figure 4.1 would be a horizontal line. Any value below the average delta_t indicates a speed-up of the crankshaft (it takes a shorter time for the next window to arrive). Any value above the average delta_t indicates a slow down of the crankshaft (it takes more time for the next window to arrive). The average angular velocity for the 1,000 rpm, 135 ft-lb run is 107.268 rad/sec. Appendix G is the MATLAB code that computes average angular velocity. The average time between pulses is 81.35 micro-seconds.

These data can be presented in any of several ways. The reciprocal of Δ_t yields the shaft speed. However, these data tend to be quite noisy. Therefore, the data will be processed and presented using the deviation in angle from a constant speed shaft.

With the ensemble averaged Δ_t 's and the average angular velocity computed, the measured response at the free end of the crankshaft can be calculated and plotted. The equation to calculate is:

$$\theta_{measured} = \theta_{known} - \bar{\omega}_{cycle} * t_{measured} \quad \text{where: } \theta_{known} = \text{angular position of optical encoder window relative to TDC}$$
$$\bar{\omega}_{cycle} = \text{average angular velocity of crankshaft}$$
$$(4.1) \quad t_{measured} = \text{time to arrival of optical encoder window}$$

Plotting the angle of the crankshaft as opposed to the angular velocity response reduces noise. Taking the integral of the angular velocity produces results that are less sensitive to noise. If the crankshaft was operating at a constant angular velocity, the response plot would be a horizontal line. Deviation from constant velocity indicates that the crankshaft angular position is leading or lagging a constant velocity phasor. Appendix G is the MATLAB code that computes measured crankshaft position deviation at the free end of the crankshaft. Figure 4.2 is a plot of measured crankshaft position deviation from a constant speed shaft.

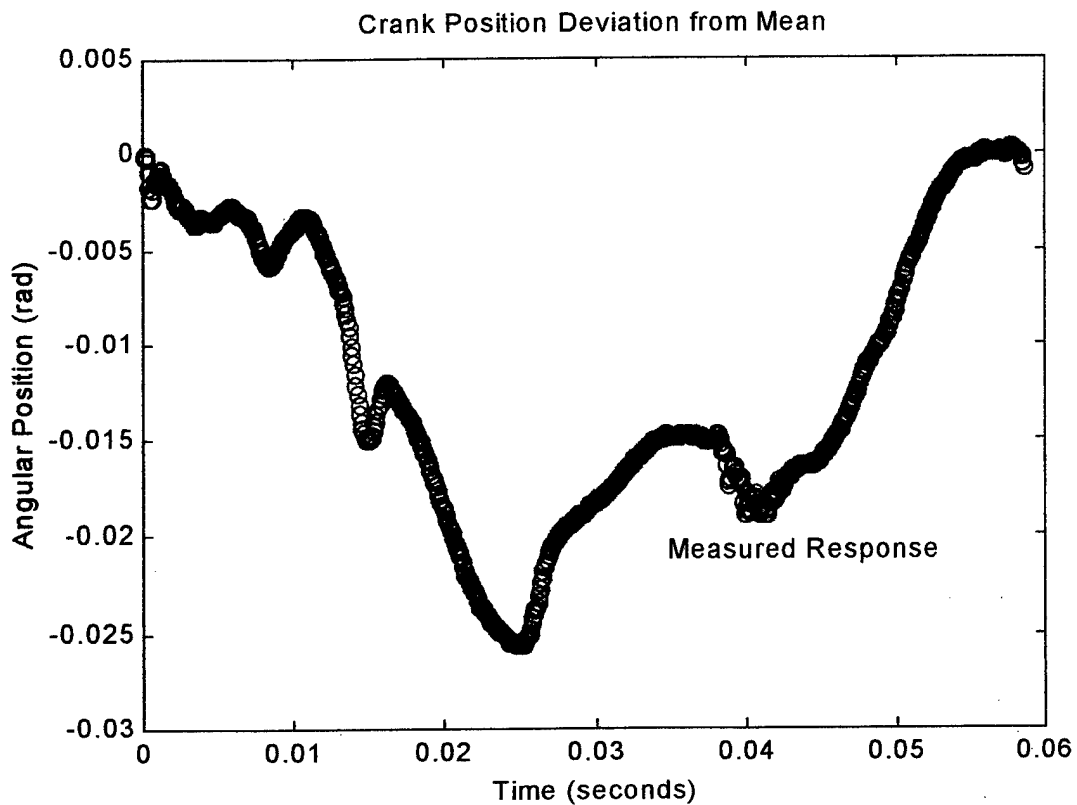


Figure 4.2 Measured Response of crankshaft at free end

B. TORSIONAL VIBRATION MODEL PREDICTED RESULTS

Utilizing the measured pressures and calculated inertia/stiffness from the model, the equations of motion were solved numerically utilizing a fourth order Runge-Kutta method. The initial conditions were: $\theta(t = 0) = 0$ rad and $\dot{\theta}(t = 0) = 108.9$ rad/sec for all degrees-of-freedom. The material damping was chosen as 0.002 and viscous damping 0.02. The non-linear reciprocating inertia terms were updated every 0.5 degrees or 720 times per revolution. The system of 12 first order differential equations was integrated from $t_{\text{initial}} = 0$ to $t_{\text{final}} = 0.058$ seconds. There were 720 linearly spaced time steps between t_{initial} and t_{final} . These time steps were chosen to match the ECA data updates. At the

completion of each time step, the response of θ_1 was recorded. Appendix G is the MATLAB code that computes predicted response. Figure 4.3 is a plot of predicted crankshaft position deviation from a constant speed shaft.

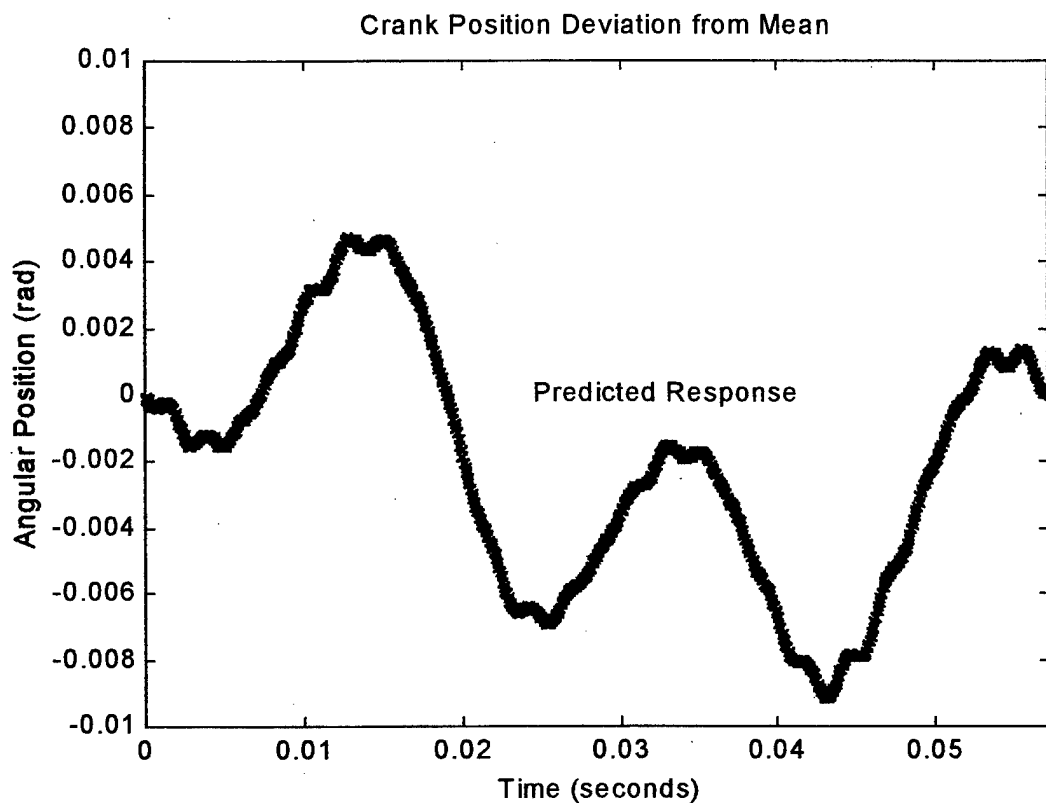


Figure 4.3 Model predicted response of crankshaft at free end

C. COMPARISON OF PREDICTED TO MEASURED RESPONSE

Figure 4.4 shows a comparison of predicted and measured response versus time. Several similarities are obvious. First, the slope reversals occur at nearly the same phase and time. Secondly, the slopes are generally the same. Measured and predicted responses show good qualitative agreement.

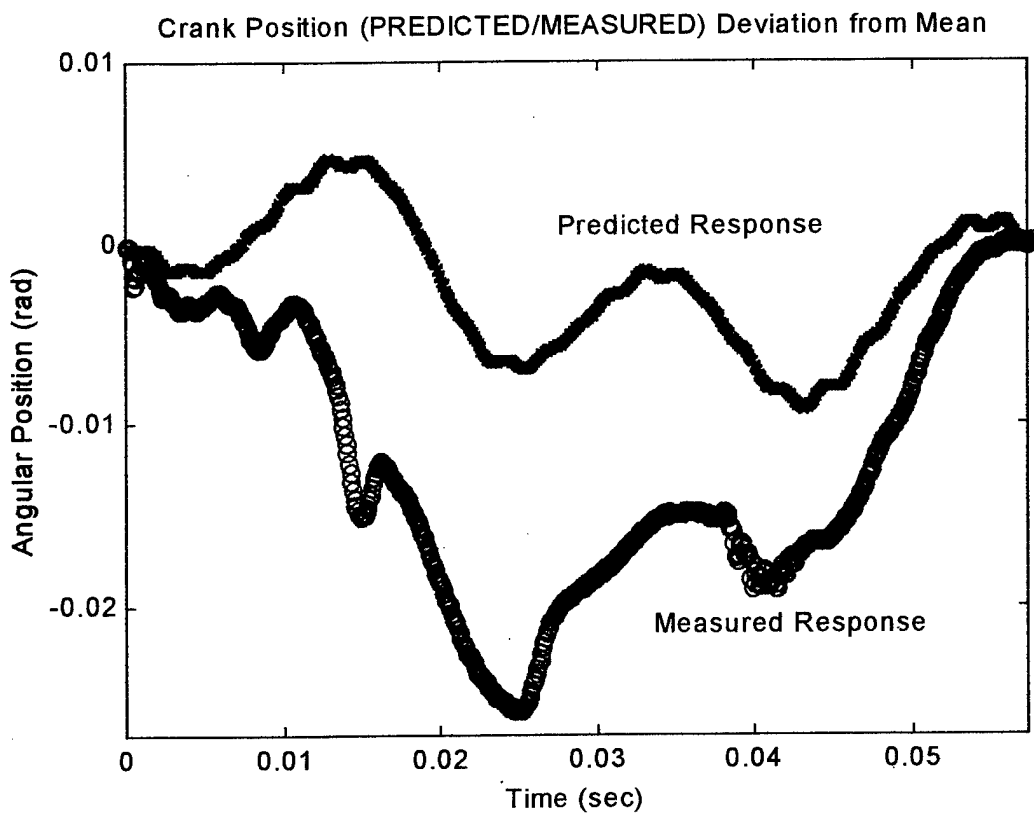


Figure 4.4 Measured and predicted responses of crankshaft at free end

To better understand these curves it is necessary to consider the driving torque. Figure 2.5 shows that the maximum gas torque for the number one cylinder occurs 20 degrees after TDC. With the crankshaft rotating at 107.3 rad/sec (1024 rpm), 20 degrees after TDC of number one cylinder occur approximately 0.0033 seconds into the cycle. The system speeds up (positive slope) until the applied torque is zero at approximately 80 degrees (0.013 seconds) after TDC. When the applied torque is zero the slope of the predicted response reverses. This pattern continues for the firings of cylinders three and two. All three distinct increases in angular velocity of the crankshaft associated with cylinders firing are clearly present.

The measured response with all of the stated similarities still has one large difference. At the beginning of the cycle, the slope decreases and continues this pattern until 0.025 seconds after TDC. After 0.025 seconds, the angular velocity increases until the cycle repeats. Examining the measured response curve indicates that the applied torque into the system is lower at the beginning of the cycle and then increases toward the end of the cycle allowing repeatability. Figure 2.5, the individual cylinder gas torque curves, show low gas torque for the number one cylinder, slightly increased gas torque for number three cylinder, and finally the greatest gas torque contribution by number two cylinder. This would appear to explain the shape of the measured response curve, low pressure in number one cylinder.

To validate the measurement, pressure transducers were interchanged between cylinders. The same pressure curves were obtained.

V. CONCLUSIONS AND RECOMMENDATIONS

A. SUMMARY

A new rigid optical encoder mount was designed and installed on the engine. A torsional vibration model was developed which included the crankshaft, major reciprocating components, and external loads. Equations of motion describing the dynamics of the system were derived. The Modulation Domain Analyzer and Engine Cycle Analyzer were used to gather time resolved information from the engine. Baseline data were obtained at eighteen different speed and torque combinations utilizing a 720 and 3,600 count optical encoder. The predicted response and the measured response were compared.

C. CONCLUSIONS

The predicted and measured response at the free end of the crankshaft show good qualitative agreement. The predicted response shows the expected increase and decrease in instantaneous angular velocity as a result of cylinders firing. The torsional vibration model with non-linear inertia and linear stiffness and damping appears to describe the dynamics of the diesel engine well. Specifically, the six degrees-of-freedom is sufficient to capture the measured torsional dynamics. Measured response appears to be different due to actual low cylinder pressure in number one cylinder.

C. RECOMMENDATIONS

The applied torque to the shaft should be calculated using a parasitic torque, where a constant magnitude is subtracted from each cylinder instead of multiplying each gas torque by the same mechanical efficiency. This should greatly improve the agreement between the model and the measurements.

Other contributions of inertia from the camshaft, counter-balance shafting, gears, and exhaust valves should be explored for significance.

More model validation can be obtained by instrumenting the flywheel with a proximeter. This adds instantaneous angular velocity information from the fifth degree of freedom. The torsional twisting between the first and fifth degrees of freedom may also hold information of interest.

The low pressure in the number one cylinder should be investigated and corrected. Once corrected, another 1,000 rpm, 135 ft-lb torque data run should be made. The measured response curve can be compared to the measured response from this research. It is expected that the results will be similar to the model predicted response.

The next step should be pressure prediction based upon instantaneous shaft speed measurement. The measured response curve could also be used to localize cylinder and engine faults.

APPENDIX A

INERTIA AND STIFFNESS FOR THE TORSIONAL ENGINE MODEL

To calculate the equivalent inertia and stiffness of the model, Reference 1 was utilized. In general, the complex system must be converted into a simpler system of equivalent masses and equivalent shafts. The manufacturer's design drawings [Ref. 9] of the crankshaft were utilized to obtain the geometry and material properties.

MASS POLAR MOMENT OF INERTIA OF CRANKSHAFT AND RECIPROCATING COMPONENTS:

1. Each equivalent mass polar moment of inertia of the crankthrows include all inertia contributions from the mid-point of a journal bearing to their left and to the their right, Figures 2.3 and 2.4 germane. The inertia from the mid-point of the front journal bearing surface to the end of the crankshaft is J_1 . It includes the inertia contribution of the optical encoder crankshaft adaptor. The inertia from the mid-point of the rear journal bearing surface to the back of the crankshaft including the flywheel is J_5 . The equivalent inertia of the water brake dynamometer is J_6 . The value of J_6 was obtained from the manufacture of the water brake [Ref. 13]. The reciprocating inertia from the pistons and connecting rods is discussed later.
2. In general, to compute the equivalent inertia of the system, the crankshaft must be broken down into simpler components. The following are the component inertias which must be summed to obtain the equivalent inertia at each degree of freedom.

a. Crankshaft journals (solid):

$$W = \frac{\pi}{4} * D_1^2 * A * \rho \text{ (lbf)}$$

$$K^2 = \frac{D_1^2}{8} \text{ (in}^2\text{)}$$

$$J = \frac{W * K^2}{g} \text{ (lbf-in-sec}^2\text{)}$$

where: W = weight of journal in lbf

K = radius of gyration of journal in inches

D₁ = diameter of journal in inches

A = length of journal in inches

ρ = specific weight of material = 0.283 lbf/in³

g = 386 in/sec²

b. Crankpins (solid):

$$\frac{D_2^2 * B}{1,735} \left[\frac{D_2^2}{8} + R^2 \right] \text{ (lbf-in-sec}^2\text{)}$$

where: D₂ = diameter of crankpin in inches

B = length of crankpin in inches

R = distance of center of gravity of crankpin
from the crankshaft axis of rotation, in inches

c. Crankwebs:

$$J = \sum \frac{W * K^2}{g} \text{ (lbf-in-sec}^2\text{)}$$

where: W = total weight of component in lbf

K = radius of gyration in inches

g = 386 in/sec²

note: Each crankweb must be broken down into small geometric shapes. The parallel axis theorem is utilized to transfer the equivalent inertia to the crankshaft axis of rotation. Table 10.13 [Ref. 1] contains radii of gyration (K) and weights (W) for 28 geometric shapes.

d. Reciprocating inertia:

$$J_{rec} = \frac{WR^2}{2 * g[1 - \cos(2\theta)]} \text{ (lbf-in-sec}^2\text{)}$$

where: W = weight of piston and connecting rod = 10.5 lbf

R = distance of center of gravity of crankpin
from the crankshaft axis of rotation, in inches

g = 386 in/sec²

θ = angular position of crankthrow after TDC

EQUIVALENT TORSIONAL STIFFNESS OF CRANKSHAFT

1. Each equivalent torsional stiffness was calculated from one degree of freedom to the next. Torsional stiffness between crankthrows is from the mid-point of the crankpin of one cylinder to the mid-point of the crankpin of the next cylinder.
2. In general, to compute the equivalent torsional stiffness of the system, the crankshaft must be broken down into equivalent lengths of shafting. Component equivalent lengths must be summed to get equivalent lengths between each degree of freedom.

a. For journals (solid), crankpins (solid), and crankwebs:

$$L_e = D^4 \left[\left\{ \frac{A + 0.4 * D_1}{D_1^4} \right\} + \left\{ \frac{B + 0.4 * D_2}{D_2^4} \right\} + \left\{ \frac{R - 0.2(D_1 + D_2)}{T * W^3} \right\} \right] \text{ (in)}$$

one journal	one pin	two crankwebs
-------------	---------	---------------

where: D = diameter of equivalent shaft in inches

A = length of journal in inches

D_1 = diameter of crank journal bearing in inches

D_2 = diameter of crankpin

R = distance of center of gravity of crankpin
from the crankshaft axis of rotation, in in.

T = thickness of crankweb in inches

W = width of crankweb in inches

* D⁴ * G

$$K = \frac{\pi^* D^* G}{32 * L_e} \text{ (lbf-in/rad)}$$

where: G = modulus of rigidity = 12.0×10^6 (lbf/in²)

b. For solid shafts:

$$K = \frac{\pi^* D^4 * G}{32 * L_e} \text{ (lbf-in/rad)}$$

c. To calculate the equivalent stiffness from crankpin to crankpin, calculate the stiffness as shown above (K_{main}). Main indicates main journal bearing surface to main journal bearing surface. $K_{\text{pin-to-pin}} = (2 * K_{\text{main}})^{-1} + (2 * K_{\text{main}})^{-1}$

- d. Figure 11.5 [Ref. 1] contains some typical crankshaft elements and equivalent lengths.

APPENDIX B

OPTICAL ENCODER AND OPTICAL ENCODER MOUNT INSTALLATION PROCEDURE

In order to obtain accurate readings from the optical encoder, the following procedure should be followed when installing the mount and or changing optical encoders:

Installing mount:

1. Place the crankshaft to optical encoder stainless steel adapter on the end of the crankshaft and firmly seat. Rotate the adapter until the two encoder shaft set screws are pointing straight up and down or vertical to the deck. Tighten the three set screws securely against the crankshaft with an allen wrench.
2. Place the smaller of the two aluminum optical encoder mounts against the engine block and then place the larger one on top oriented such that the encoder will mate. Obtain the optical encoder mount bolts and hand tighten the bolts until the mounts are flush with the block. Figure 3.2 shows this orientation.
3. Obtain the optical encoder alignment jig. Place it into the countersunk encoder receptor. The purpose of the jig is to align the mount so the crankshaft rotates concentrically with the optical encoder shaft. Carefully tighten down all three optical encoder mounting bolts. Ensure that the jig is able to move in and out of the encoder adapter hole and the mounting lip without binding. It may be necessary to shim the encoder mount. If all three bolts are securely fastened and the jig moves in and out freely from the receptor, the optical encoder mount is aligned.

Installing optical encoder:

1. Place optical encoder into the receptor and install the three small bolts which retain it. Tighten the bolts with an allen wrench.
2. On the bottom of the optical encoder there is a window which allows access to the encoder shaft set screws. Tighten the one set screw securely against the optical encoder shaft with an allen wrench. It may be necessary to utilize a flashlight and mirror to accomplish this.
3. Remove the access plate over the flywheel. Rotate the engine crankshaft clockwise with a pry bar 180 degrees. This allows the other the set screw to be accessed.
4. Tighten the remaining set screw securely against the optical encoder shaft with an allen wrench.

The optical encoder mount and optical encoder are now aligned. Ensure that TDC relative to the optical encoder is established prior to engine operation, Appendix G germane.

APPENDIX C

ESTABLISHING REFERENCE PRESSURE

In order to obtain the most accurate cylinder pressure readings, the ECA requires a reference pressure input. This appendix describes the procedure for establishing reference pressure versus speed. It is obtained at normal operating temperature of the engine.

An MKS Instruments Inc. Type 698 differential high-accuracy pressure transducer in conjunction with the MKS Instruments Inc. Signal Conditioner Type 270B was used to measure engine air box pressure relative to atmospheric pressure. The range of the differential pressure transducer was 1,000 torr (20 psi), sufficient to measure the air box pressure. The Air box pressure was obtained by removing a cold weather spark plug on the side of the engine and using the threaded hole for a air box pressure tap. The other side of the differential pressure transducer was open to the atmosphere. The engine was operated from 700 to 2,500 rpm in increments of 200 rpm. At every increment of speed, the air box pressure was recorded. A plot of reference air box pressure versus engine speed was constructed, Figure 3.3 germane. When measuring cylinder firing pressures, the reference air box pressure for the speed of engine operation should be input into the ECA set up file.

The following picture shows the set up of the pressure transducer, signal conditioner, and associated piping to the engine.

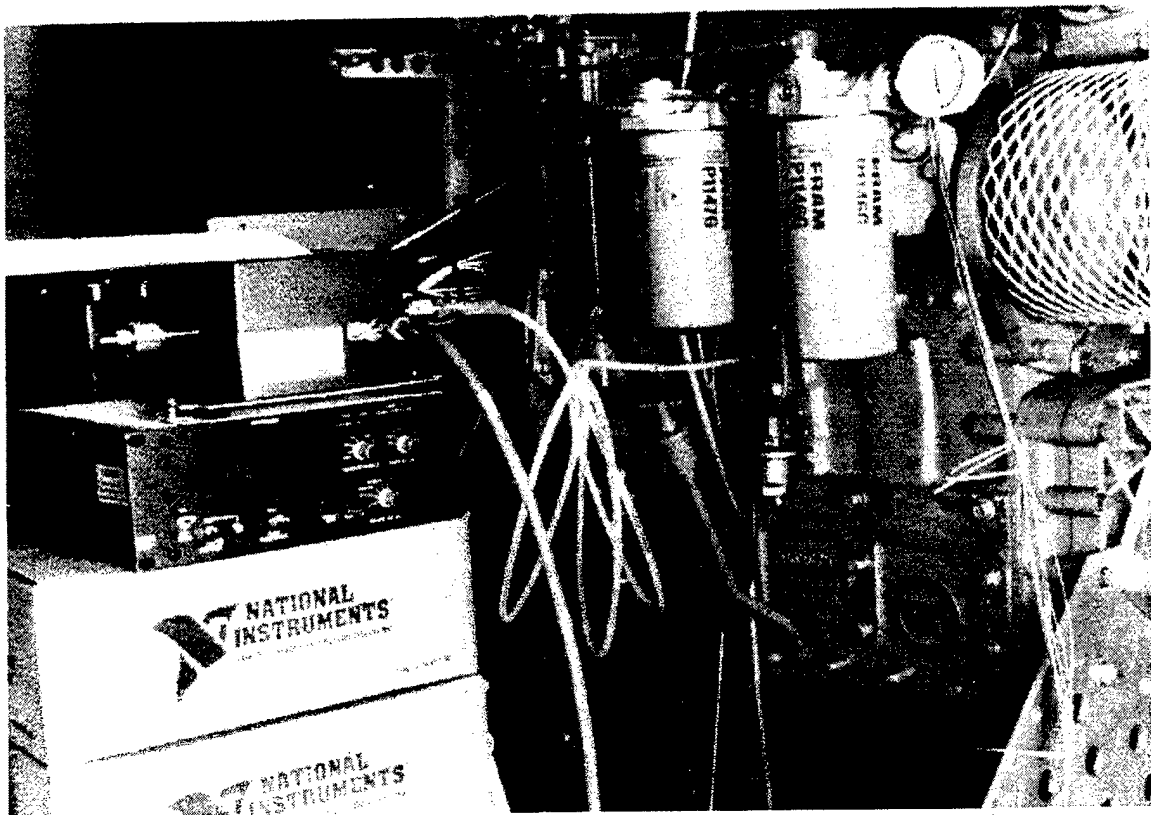


Figure C.1 Instrumentation utilized for establishing reference air box pressure versus engine speed.

APPENDIX D

MODULATION DOMAIN ANALYZER OPERATING PROCEDURE

This appendix describes how to configure and operate the modulation domain analyzer (MDA) to record time resolved information from the optical encoder during engine operation. The procedure is:

1. Ensure both the MDA and data acquisition computer are turned off.
2. Connect one end of the IEEE-488 cable (National Instruments 763061-02 Rev C, Type-X2, Length 2.1 meter) to the HPIB on the back side of the MDA. Connect the other end of this cable to the National Instruments GPIB board interface on back of the data acquisition computer.
3. Connect the TDC output on front of the ECA sensor interface to the EXT Arm input on front of the MDA with a BNC connector.
4. Connect the CA output on front of the ECA sensor interface to the Channel A input on front of the MDA with a BNC connector.
5. Turn the power to the MDA on.
6. Depress the 'function and input' menu key.
7. Select the 'time interval' soft key.
8. Select 'common' A and B line soft key.
9. Select 'rising edge A and Rising edge B' soft key.
10. Depress the 'trigger' menu key.
11. Select 'triggered' soft key.
12. Select 'mean' and '1/mean' on the entry panel to display the mean δ_t and mean frequency.
13. Start the engine in accordance with Appendix A [Ref. 1].
14. Depress the 'auto scale' menu key.
15. The MDA is now displaying δ_t on the y-axis and time on the x-axis. Continue with step 16 to make the MDA ready for remote operation and data acquisition.
16. Turn on the power to the data acquisition computer and go to the HP Applications icon and enter.
17. For remote operation, depress the 'utility' menu key on the MDA.
18. Select 'addressed' under the HP-IB/Print soft key.
19. Select address number 5 (five).
20. The MDA is now in remote operation mode. **In order to print the screen or operate the MDA locally, the 'TALK ONLY' mode must be enabled.**

The following section discusses how to access the memory of the MDA, record the measured Δ_t 's, and store this information with the data acquisition computer.

1. With the MDA properly configured, select the HP Applications icon and go to the HP53305A Phase Analyzer software. Connect 'CA' lead to 'B' input on MDA.
2. Under the setup menu, select instrument setup and configure the following:
 - a. Input configure: B, + slope, DC coupling, and 50 ohm impedance.
 - b. Arming: EXT, TTL, and + slope.
 - c. Interface: National GPIB, 0 board index, and address 5.
4. Under the setup menu, select measure/view setup and configure the following:
 - a. Parameter: Frequency and Phase.
 - b. Number of samples: Enter the number of sample points desired for the run but do not exceed 32,000. Remember, the 720 count optical encoder is 720 data samples/revolution and the 3,600 optical encoder is 3,600 samples/revolution.
 - c. Measurement time: Enter the approximate expected Δ_t 's expected for the speed you are taking data at. (i.e. at 1000rpm, with the 720 optical encoder, enter 83.3 microseconds or
$$\frac{\text{min}}{1,000\text{rev}} * \frac{\text{rev}}{720\text{windows}} * \frac{60\text{ sec}}{\text{min}}$$
).
 - d. Number of averages: one.
 - e. Pacing: auto.
 - f. Input: B.
 - g. Clock/carrier frequency: calculated.
 - h. No filter.
5. Under the setup menu, select phase units then select 'unit interval'.
6. The MDA is now ready to collect TDC triggered data from the optical encoder.
7. When ready to start collecting data, go to the measure menu and select 'phase deviation'. As soon as you release the mouse button, the MDA records data.
8. Once the data is recorded, the MDA will ask you what to name the plot. This is unimportant, enter anything.
9. Save the data to the hard drive or zip drive as a M-File.
10. With MATLAB, remove the header and footer information which leaves two columns of numbers. The length of the array is the number of sample points you previously selected during setup of the software.
11. The data file is now ready for use by MATLAB code, Appendix H germane.



Figure D.1 MDA and high speed data acquisition computer. An oscilloscope sets on top of the MDA.

APPENDIX E

DATA ACQUISITION PROCEDURE

This appendix describes the data acquisition procedure for comparing model predicted response to measured response at the free end of the crankshaft utilizing the 720 count optical encoder. The procedure is:

1. Align the engine for operation and turn the charge amplifiers on. Ensure the proper scale and sensitivity is set on charge amplifiers. This information is on the Kistler pressure transducer calibration sheets.
2. Setup the ECA setup file used for data acquisition in accordance with Appendix F.
3. Align the MDA and data acquisition computer in accordance with Appendix D.
4. Increase the engine and load to the desired set point.
5. On the ECA, select data taking and statistics under the main menu.
6. Select 720DD353.SET under the data taking and statistics menu. 720DD353.SET is the preset for monitoring and recording all three cylinder pressures utilizing the 720 count optical encoder. DD353PRE.SET is the setup file for monitoring and recording all three cylinder pressures utilizing the 3,600 count optical encoder.
7. Enter the correct reference pressure from Figure 3.3 into the J.1 block and enter the number of cycles to be samples (should correspond with the MDA).
8. Place the charge amplifiers in the 'operate' mode.
9. Enter 'G' for graphic monitoring and ensure three pressure versus theta curves appear.
10. The ECA is now ready to record data.
11. The ECA will temporarily turn on and off the output crank angle and TDC signals while it is acquiring data. Therefore, the MDA data must be taken first.
12. Record the speed and torque of the engine by depressing 'Record Data' on the SuperFlow Dynamometer Control Console.
13. Take the MDA measured data in accordance with Appendix D.
14. Immediately after the MDA data acquisition data is taken, depress "D" for data taking on the ECA keyboard. Follow on screen instructions.
15. Store each individual cylinder pressure to the hard drive.
16. Data acquisition is complete. Steps 12 through 15 above require practice and should be accomplished as fast as possible to avoid any deviation in speed and torque from the engine.

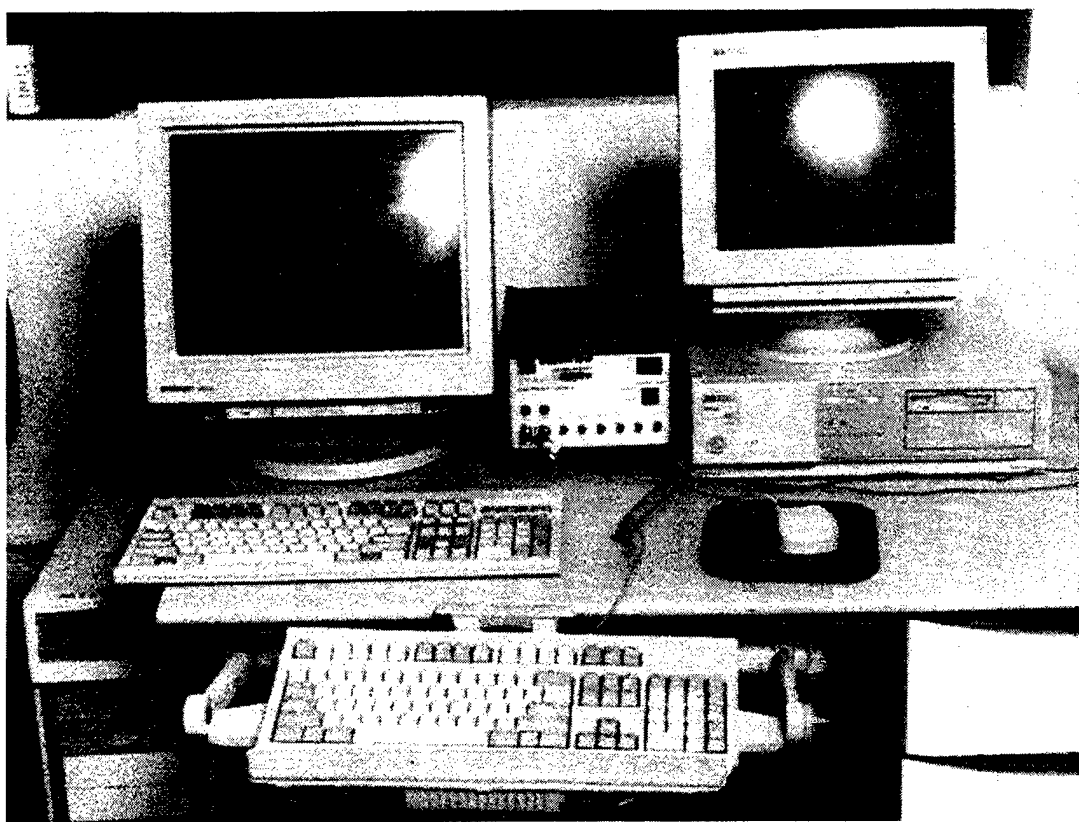


Figure E.1 ECA, ECA sensor interface, and SF-901 Dynamometer computer.



Figure E.2 SuperFlow Dynamometer Control Console

APPENDIX F

ESTABLISHING TOP DEAD CENTER RELATIVE TO THE OPTICAL ENCODER

In order to get accurate readings from the optical encoder, the following procedure should be followed to correctly position Top Dead Center (TDC) of the number one cylinder relative to the optical encoder. TDC is the reference against which all angular measurements are made. It is the point in the cycle of a cylinder when the volume is the least. The number one cylinder is the cylinder for this reference. The procedure outlined in Appendix G of Reference 1 is unchanged with the following exceptions.

1. To rotate the engine, remove the flywheel access cover on the back of the engine.
2. A pry bar, as the one depicted, can be utilized to rotate the engine.
3. Once mechanical TDC of the number one cylinder is established, loosen the three retaining bolts that secure the optical encoder to the mount.
4. Rotate the optical encoder until the TDC signal on the ECA sensor interface illuminates.
5. Carefully tighten the retaining bolts on the optical encoder base.

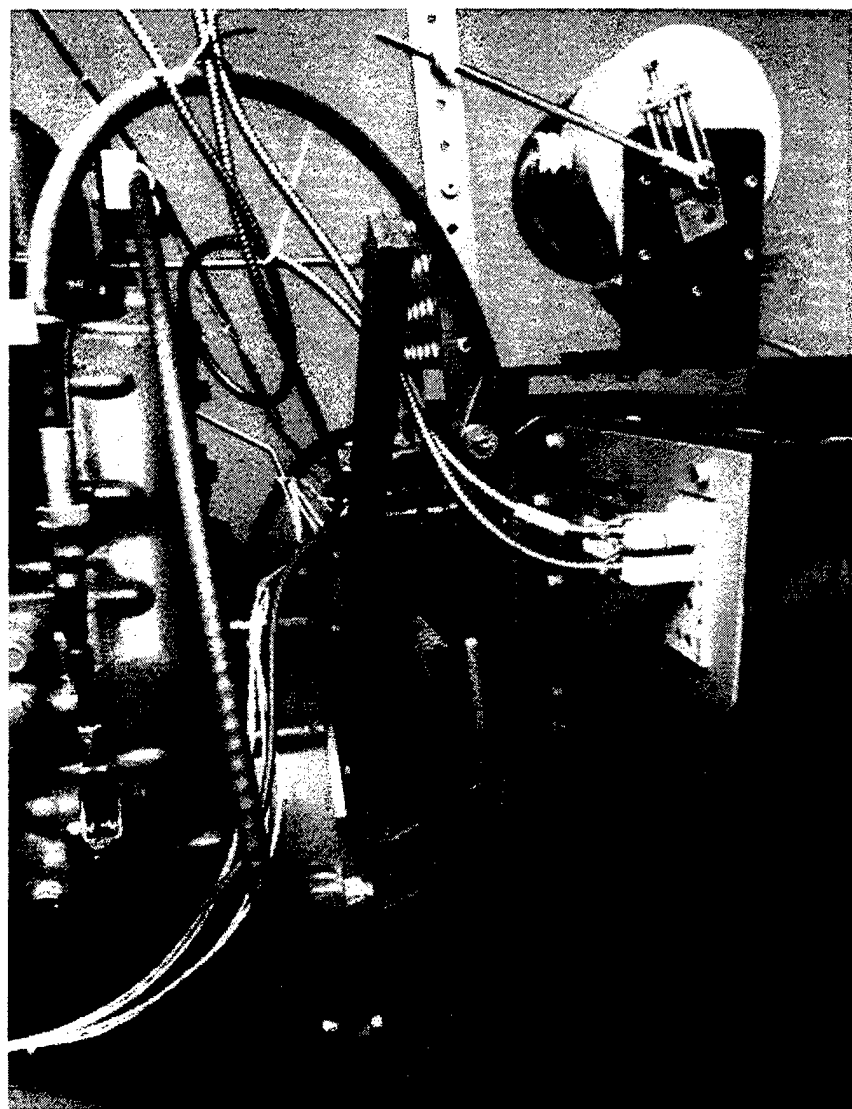


Figure F.1 Flywheel access cover removed with pry bar in place.

APPENDIX G

MATLAB CODE USED FOR CYCLE ANALYSIS

This Appendix contains all the different MATLAB M-files used for this research. Data from both the ECA and MDA require that the footer and header information be removed prior to loading into an M-file. The ECA records data pressure from -180 degrees to 180 degrees relative to TDC. Before loading the ECA data into an M-file for analysis, it must first be rearranged and saved from 0 degrees to 360 degrees after TDC. This procedure must be followed for each cylinder pressure data.

The following code can be utilized to:

- a. Plot pressure versus crank angle for all three cylinders.
- b. Plot gas torque versus crank angle for all three cylinders.
- c. Compute average gas torque contribution from each cylinder
- d. Compute the mechanical efficiency based upon a torque balance.
- e. Compute and plot the phase lock, ensemble average of MDA raw data.
- f. Compute the average angular velocity through each revolution from MDA data.
- g. Solve the equations of motion of the system and plot a predicted response at the free end of the crankshaft.
- h. Compute and plot the measured response at the free end of the crankshaft utilizing MDA phase lock, ensemble average data.

I. Define the equations of motion as a system of 12 first order differential equations.

```

% This code computes and plots the Individual cylinder pressures
% Referenced to Nr. 1 cylinder TDC
% Filename: cylpress.m
load d15kr135.m % ECA cylinder #1 pressure data
load e15kr135.m % ECA cylinder #2 pressure data
load f15kr135.m % ECA cylinder #3 pressure data
%
%PLOTS PRESSURE OF EACH INDIVIDUAL CYLINDER VS DEGREES AFTER TDC OF NR1 CYL
%
theta=1:1:720;
plot(theta/2,(d15kr135(theta)*14.5),'x',theta/2,(e15kr135(theta)*14.5),'o',theta/2,(f15kr135(theta)*14.5),'-')
title('Individual Cylinder Pressure referenced to TDC of Nr. 1 cylinder')
xlabel('Degrees after TDC of Nr. 1 Cylinder')
ylabel('Pressure (PSI)')
legend('Nr 1 cyl pressure','Nr 2 cyl pressure','Nr 3 cyl pressure')
axis([-inf 361 0 1250])

%
% This code computes the individual torque contribution of each
% individual cylinder referenced to TDC of Nr.1 Cylinder and the
% reciprocating inertia. It can also be manipulated to plot
% pressure vs. theta curves
% Filename: torque.m
%
load d1kr135.m % ECA cylinder #1 pressure data
load e1kr135.m % ECA cylinder #2 pressure data
load f1kr135.m % ECA cylinder #3 pressure data
r=2.25;W=10.5;g=386; %constants
for theta=1:720
    T1cyl(theta)=(d1kr135(theta)*14.5*r*sin(theta*.008726646)*(pi*r^2))/12; % FT-LB
    T2cyl(theta)=(e1kr135(theta)*14.5*r*sin((theta*.008726646)-(4*pi/3)*(pi*r^2))/12;% FT-LB
    T3cyl(theta)=(f1kr135(theta)*14.5*r*sin((theta*.008726646)-(2*pi/3)*(pi*r^2))/12;% FT-LB
    j2rec(theta)=(W*r^2/(2*g))*(1-cos(2*(theta*.008726646))); %lb*in*sec^2
    j3rec(theta)=(W*r^2/(2*g))*(1-cos(2*(theta*.008726646)-(2*pi/3))); %lb*in*sec^2
    j4rec(theta)=(W*r^2/(2*g))*(1-cos(2*(theta*.008726646)-(4*pi/3))); %lb*in*sec^2

    % plot(theta/2,(T1cyl+T2cyl+T3cyl),'kX')
    % title('Net Torque Input Referenced to TDC of Nr. 1 Cylinder')
    % xlabel('Degrees after TDC of Nr. 1 Cylinder')
    % ylabel('Gas Torque (FT-LB)')
    % hold on
end
figure(1)
theta=linspace(1,720,720);
plot(theta/2,T1cyl,'X',theta/2,T2cyl,'O',theta/2,T3cyl,'-')
title('Individual Cylinder Torque input Referenced to TDC of Nr. 1 Cylinder')
xlabel('Gas Torque (FT-LB)')
ylabel('Degrees after TDC of NR. 1 Cylinder')

```

```

legend('Nr 1 Cyl Torque','Nr 2 Cyl Torque','Nr 3 Cyl Torque')
figure(2)
plot(theta/2,j2rec,'X',theta/2,j3rec,'O',theta/2,j4rec,'.')
title('Individual Reciprocating Crankthrow Inertia Referenced to TDC of Nr.1 Cylinder')
xlabel('Inertia (lb*in*sec^2)')
ylabel('Degrees after TDC of Nr. 1 Cylinder')
legend('Nr 1 Cyl Reciprocating Inertia','Nr 2 Cyl Reciprocating Inertia','Nr 3 Cyl Reciprocating Inertia')

```

```

%
% THIS SECTION COMPUTES THE AVERAGE TORQUE CONTRIBUTION OF EACH CYLINDER
%
tic
x=linspace(0,(2*pi),720);
T1cyl_avg=trapz(x,T1cyl)/(2*pi)
T2cyl_avg=trapz(x,T2cyl)/(2*pi)
T3cyl_avg=trapz(x,T3cyl)/(2*pi)
Avg_Torque_input=(T1cyl_avg+T2cyl_avg+T3cyl_avg)/3
Torque_out_to_Torque_in=134/(T1cyl_avg+T2cyl_avg+T3cyl_avg)

```

```

% Jim Hudson Thesis file
% 720 OE, SAMPLE RUN 1000 RPM, 135 FT-LB TORQUE
% 16 NOV 1997 Filename: ensemble.m
% 31680 sample points from MDA or 44 revs of INFO
% THIS CODE PHASE LOCKS AND ENSEMBLE AVERAGES
% THE OUTPUT REPRESENTS ONE REVOLUTION OF INFO
load 71kr135.m % This is where the 31680 times are located
t=X71kr135(:,1); % Assigns vector "t" to each time sample
for b=1:31680
    tt(b)=t(b+1)-t(b); % Computes the del_T's and assigns
end % them to Vector "tt"
tt=(reshape(tt,720,44))'; % Phase locks and adds
ttt=sum(tt)/44; % Averages the phase lock
position=linspace(0,(2*pi),720);
timer=0; % Initialize a counter
for e=1:720
    time=[e;t(e+1);ttt(e)];
    plot(timer,ttt(e),'kX') %PLOTS TIME VS. DEL_T
    timer=timer+ttt(e);
    hold on
end
gtext('1000 RPM & 135 Ft-Lbs, 720 Optical Encoder')
title('MDA DATA PHASE LOCK ENSEMBLE AVERAGED')
ylabel('Delta_t btwn windows (Seconds)')
xlabel('Time of sample, after TDC (SECONDS)')

```

```

% This code computes the average angular velocity through each
% of the 44 revolutions of of MDA data. Additionally, it gives

```

```

% the average angular velocity the MDA saw.
% filename: omegacyc.m
%
load 71kr135.m      % This is where the MDA raw data is stored
for a=1:31681
    t(a)=X71kr135(a);
end
for n=1:44
    x(n)=720*n;
end
omega_zero=(2*pi)/(t(720)-t(1));
plot(0,omega_zero,'kX')
hold on
sum=omega_zero;
for c=1:43
    omega_avg(c)=(2*pi)/(t(x(c+1))-t(x(c)+1));
    sum=sum+omega_avg(c);
end
c=linspace(1,43,43);
average=sum/44      % This is the average angular velocity
plot(c,omega_avg,'kX')
title('Average Angular Velocity Through Each of the 44 Revolutions')
xlabel('Cycle Number')
ylabel('Average Angular Velocity (rad/sec)')

```

```

% THIS CODE PLOTS CONCURRENTLY THE MEASURED AND PREDICTED RESPONSES
% for a 720 count optical encoder. The measured and predicted
% response can be plotted independently by simply commenting out
% one or the other. Filename: measpred.m
% 31680 sample points from MDA are located in file: 71KR135.M
% ECA cylinder pressure information is in files:
% d1kr135.m cylinder #1 pressure data
% e1kr135.m cylinder #2 pressure data
% f1kr135.m cylinder #3 pressure data
%
% This first section plots the measured response
%
load 71kr135.m      % THIS IS WHERE THE 31680 TIMES ARE LOCATED
t=X71kr135(:,1);    % ASSIGNS VECTOR "t" TO EACH TIME SAMPLE
for b=1:31680
    tt(b)=t(b+1)-t(b); % COMPUTES THE DEL_T'S AND ASSIGNS THEM TO
end                  % VECTOR "tt"
tt=(reshape(tt,720,44))';% This phase locks one cycle
tttt=sum(tt)/44;        % This ensemble averages the phases
position=linspace(0,(2*pi),720); % The known positions of the O.E. windows
timer=0;
for e=1:720
    plot(timer,(position(e)-(107.278*timer)), 'rO') %107.278 is omega_bar
    timer=timer+tttt(e);
    hold on
end

```

```

gtext('Measured Response')
hold on
%
% This section is a SIX SECOND ORDER SUMULTANEOUS EQUATION ODE SOLVER
% This section calls "eqns.m" which defines the system of 2nd order ode's
%
global Tload p1cyl p2cyl p3cyl T1cyl T2cyl T3cyl ...
j2rec j3rec j4rec j1 j2 j3 j4 j5 j6 k1 k2 k3 k4...
k5 c12 c23 c34 c45 c56 c2 c3 c4 %share the variables with other m-files
ic=[0 0 0 0 0 108.909 108.909...
108.909 108.909 108.909 108.909]; %define IC's [x(t=0) & xdot(t=0)]
load dlkr135.m % cylinder #1 pressure data from the ECA
load elkr135.m % cylinder #2 pressure data from the ECA
load flkr135.m % cylinder #3 pressure data from the ECA
Tload=1608; % lb-in (134 FT-LB as measured by the dynamometer)
z=linspace(0,.057692066,721); % divide .058 secs into 720 evenly
% spaced time increments
r=2.25; % Crankshaft eccentricity (in)
W=10.5; % The weight of the reciprocating components
% (piston and connecting rod) (lbf)
g=386; % The acceleration of gravity (in/sec^2)
mech_eff=.6175; % This is the scale factor for the Gas Torque in
% mech_eff=Tload/(T1avg+T2avg+T3avg)
% M-file Torque.m computes the gas torques
omega_bar=109.9; %This is the mean speed of the crankshaft used
%by the plot command for "Response Deviation"
j1=.0291; %lb*in*sec^2/rad
j2=.2730; %lb*in*sec^2/rad
j3=.1710; %lb*in*sec^2/rad
j4=.2730; %lb*in*sec^2/rad
j5=6.194; %lb*in*sec^2/rad
j6=.2800; %lb*in*sec^2/rad
k1=3.470e6; %lb*in/rad
k2=9.551e6; %lb*in/rad
k3=9.551e6; %lb*in/rad
k4=13.495e6; %lb*in/rad
k5=1.304e6; %lb*in/rad
c12=.002; %lb*in*sec/rad
c23=.002; %lb*in*sec/rad
c34=.002; %lb*in*sec/rad
c45=.002; %lb*in*sec/rad
c56=.002; %lb*in*sec/rad
c2=.02; %lb*in*sec/rad
c3=.02; %lb*in*sec/rad
c4=.02; %lb*in*sec/rad
x=ic; %Initialize the "x" vector to compute Tcyl's and Jrec's
for theta=1:720
T1cyl=mech_eff*dlkr135(theta)*14.5*r*sin(theta*.008726646)*(pi*r^2);%lb-in
T2cyl=mech_eff*elkr135(theta)*14.5*r*sin((theta*.008726646)-(4*pi/3))*(pi*r^2);%lb-in
T3cyl=mech_eff*flkr135(theta)*14.5*r*sin((theta*.008726646)-(2*pi/3))*(pi*r^2);%lb-in
j2rec=(W*r^2/(2*g))*(1-cos(2*theta*.008726646)); %lb*in*sec^2
j3rec=(W*r^2/(2*g))*(1-cos(2*(theta*.008726646)-(2*pi/3))); %lb*in*sec^2
j4rec=(W*r^2/(2*g))*(1-cos(2*(theta*.008726646)-(4*pi/3))); %lb*in*sec^2

```

```

[T,x]=ode45('eqns',z(theta),z(theta+1),ic);
  ic=x(length(T),:); % REINITIALIZE THE IC'S FROM THE PREVIOUS ITERATION
  plot(T(length(T)),x(length(T),1)-(omega_bar*T(length(T))),'bX')
end
title('Crank Position (PREDICTED/MEASURED) Deviation from Mean')
xlabel('Time (sec)')
ylabel('Angular Position (rad)')
axis([0 .0573 -.027 .01]) % Change this for the appropriate desired view
gtext('Predicted Response')

% This code defines the 12 first order equations to be differentiated.
% FILENAME: EQNS.M
function xdot=firsteqn(t,x,Tload)
global Tload T1cyl T2cyl T3cyl j2rec j3rec j4rec j1 j2 j3...
j4 j5 j6 k1 k2 k3 k4 k5 c12 c23 c34 c45 c56 c2 c3 c4
%
% These are 12 first order equations which define the
% original 6 second order equations of motion!!!!
%
xdot(1)=x(7);
xdot(2)=x(8);
xdot(3)=x(9);
xdot(4)=x(10);
xdot(5)=x(11);
xdot(6)=x(12);
xdot(7)=(c12*x(8))-(c12*x(7))+(k1*x(2))-(k1*x(1))/j1;
xdot(8)=(T1cyl+(c23*x(9))-(c23+c12+c2)*x(8))+(c12*x(7))+(k2*x(3))...
-((k1+k2)*x(2))+(k1*x(1))/(j2+j2rec);
xdot(9)=(T2cyl+(c34*x(10))-(c34+c23+c3)*x(9))+(c23*x(8))+(k3*x(4))...
-((k2+k3)*x(3))+(k2*x(2))/(j3+j3rec);
xdot(10)=(T3cyl+(c45*x(11))-(c45+c34+c4)*x(10))+(c34*x(9))+(k4*x(5))...
-((k3+k4)*x(4))+(k3*x(3))/(j4+j4rec);
xdot(11)=((c56*x(12))+(c56+c45)*x(11))+(c45*x(10))+(k5*x(6))...
-((k4+k5)*x(5))+(k4*x(4))/j5;
xdot(12)=(-Tload-(c56*x(12))+(c56*x(11))-(k5*x(6))+(k5*x(5)))/j6;
xdot=xdot'; % THIS IS THE VECTOR DEFINING THE EQUATIONS OF MOTION

```

LIST OF REFERENCES

1. Wilson, W. K., "Practical Solution of Torsional Vibration Problems," Third Edition Revised, pp. 499-661, John Wiley & Sons Inc., 1956.
2. Kabele, D. F., "A New Approach in the Simulation of Crankshaft Torsional Vibration," Society of Automotive Engineers Paper Number 844140, 1984.
3. Citron S. J., O'Higgins J. E., Chen L. Y., "Cylinder by Cylinder Engine Pressure and Pressure Torque Waveform Determination Utilizing Speed Fluctuations," Society of Automotive Engineers Paper Number 890486, 1989.
4. Rizzoni, G., "Diagnosis of Individual Cylinder Misfires by Signature Analysis of Crankshaft Speed Fluctuations," Society of Automotive Engineers Paper Number 890884, 1989.
5. Sobel J. R., Jeremiasson J., Wallin C., "Instantaneous Crankshaft Torque Measurement in Cars," Society of Automotive Engineers Paper Number 960040, 1996.
6. Brown T. S., Neill W. S., "Determination of Engine Cylinder Pressures from Crankshaft Speed Fluctuations," Society of Automotive Engineers Paper Number 920463, 1992.
7. Bell, J. E., "Assessment of Diesel Engine Condition Using Time Resolved Measurements and Signal Processing," Naval Postgraduate School, Monterey CA, M.Sc. Thesis, Sep. 1996.
8. Detroit Diesel, Equivalent Mass Elastic System 3-53 Engine, Official Correspondence, May 1997, Detroit Diesel Corporation.
9. Detroit Diesel Series 3-53 Crankshaft Dimensions, 1957, Detroit Diesel Corporation.
10. Detroit Diesel Engines, Series 3-53 Service Manual, May 1990, Detroit Diesel Corporation.
11. Detroit Diesel, Series 3-53 N. A. Performance Information and Peak Firing Pressure, Facsimile, Aug 1996, Detroit Diesel Corporation.
12. Armstrong, R. A., "Fault Assessment of a Diesel Engine Using Vibration Measurements and Advanced Signal Processing," Naval Postgraduate School, Monterey CA, M.Sc. Thesis, Dec. 1996.

13. SuperFlow, Inertia Data for Water Brake Dynamometer, Facsimile, Aug 1997,
SuperFlow Corporation.

INITIAL DISTRIBUTION LIST

1. Defense Technical Information Center.....2
8725 John J. Kingman Rd., STE 0944
Ft. Belvoir, VA 22060-6218
2. Dudley Knox Library.....2
Naval Postgraduate School
411 Dyer Rd.
Monterey, Ca 93943-5101
3. Department Chairman, Code ME.....1
Department of Mechanical Engineering
Naval Postgraduate School
Monterey, CA 93943-5101
4. Professor Knox T. Millsaps Jr., Code ME/MI.....4
Department of Mechanical Engineering
Naval Postgraduate School
Monterey, CA 93943-5101
5. Curricular Officer, Code 34.....1
Department of Mechanical Engineering
Naval Postgraduate School
Monterey, CA 93943-5101
6. Detroit Diesel Corporation.....1
Mr. Kent Gregorius
13400 Outer Drive, West
Detroit, MI 48239-4001
7. Mr. Ron Hudson.....1
880 Woodland Ave.
Corydon, IN 47112
8. LT James W. Hudson.....3
313 Davis St.
Portsmouth, RI 02871